Root and leaves growth differentially respond to soil mineral content and microbiota

Valéria dos Santos Custódio

Supervisor: Dr. Gabriel Castrillo

Dissertation presented to obtain the Master of Research degree

School of BioSciences | University of Nottingham

Nottingham, July 2021

To my family

Acknowledgement

The realisation of this thesis would not be possible without the support of essential people.

To my father, Osvaldo, and mama “prossora”, a deeply thank you for always being present despite the distance. All I’ve achieved so far was by wanting to be like you. To my uncle, Valério, that wherever he is, his support and affection are unconditional.

To Gabriel Castrillo, a supervisor, a mentor, and more importantly, a good friend. My special thank you and gratitude for the opportunity to be at your lab, where your vision and approach to science have shown me that dedication, discipline, transparency, audacity and creativity are important values to achieve excellence in science. I hope one day, I will be an excellent scientist as you are.

To Isai Salas-González, for not only teaching me how to analyse all this complex data but also for getting my back when data analysis was too much for me to handle. A special thank you as well for always having the appropriate advice to help me find my way.

To Paulina Flis, for being an excellent chemical analyst that I always trust my ionome analysis. Notably, a special thank you for your support and friendship. I learned every day how to be a good person and a good friend.

To my best friends Carmen Garcia, Claudete Neves and Claudinete Neves for all your support and, more important, for the embrace and love of my good, bad and villain beings.

To my colleagues, Guillem Reyt, Riccardo Fusi, Niokhor Bakhoum, Mathieu Gonin and Elina Chrysantheou, for their friendship, support and dedication.

And of course, a big thank you to everyone in Plant Sciences and Glasshouse team for all their support that makes my work go as smoothly as possible.

To everyone here, thank you very much.

Valéria Custódio

Abstract

Plants integrate complex regulatory networks to ensure the adaptative growth of roots and leaves. These networks combine internal signals and external cues, such as nutrient availability and plant-colonising microorganisms – plant microbiota. The extent to how microbial communities, nutrient availability and internal signalling are coordinated to ensure adaptative growth of plant organs remains poorly understood. To study root and leaf responses to the different environmental cues, we planted four maise genotypes in three selected soils with different mineral nutrient contents and bacterial compositions. While root growth of the different genotypes was not affected by soil variability, leaves differentially integrated the soil effect. To understand the factors modulating the development of individual leaves, we investigated their mineral nutrient content and microbiome composition. We demonstrated that the soil effect on leaf development results from changes in the concentration of individual mineral elements impacting distinct leaf-associated bacterial communities.

Index

List of Figures

1 Introduction

In nature, plants integrate different mechanisms to ensure the adaptative growth of roots and leaves in response to environmental changes (Martins et al., 2017; Peng et al., 2021; Rao et al., 2021). This response occurs through complex regulatory networks that integrate internal signals (genetic) and external cues, such as nutrient availability, soil water content, light, pathogens, and beneficial bacteria (De Wit et al., 2016; Durán et al., 2018; Vega et al., 2019; Gu et al., 2020). Recent evidence suggests that these external cues may differentially affect the growth of roots and leaves. For instance, magnesium (Mg) deficiency impaired root and leaf growth in potato (*Solanum tuberosum* L.) (Koch et al., 2020), while iron and ammonium induce adventitious root formation in leaf cuttings of *Petunia hybrida* (Hilo et al., 2017). However, in most of these studies, the plant-associated microbial diversity, the plant microbiota, that contribute to host nutrition, development and growth (Hiruma et al., 2016; Castrillo et al., 2017; Harbort et al., 2020a) was not taken into consideration. Therefore, little is known about how plant organs ensure their growth when the microbiota is present and how the plants integrate the microbiota effect in their responses to environmental stressors.

1.1 Plant growth and regulation

Organ development is a dynamic process of progressive specialization of cells and tissues that determine organ growth and the rate at which developmental processes occur (Kalve et al., 2014). Plant organs are formed post-embryonically and emerge from an organized cluster of dividing cells known as meristems (Stahl and Simon, 2010; Sablowski, 2011). Two main meristems are specified during embryogenesis which are responsible for almost all the growth that occurs post-embryonically: the shoot apical meristem (SAM), which gives rise to above-ground tissues and organs (Du et al., 2018) and the root apical meristem (RAM), which establishes the root architecture (Motte et al., 2019).

1.1.1 Leaf growth and regulation

In plants, leaf development follows a general program that is flexible and adjusts according to species, developmental stages, and in response to

environmental factors (Poethig, 2013; Bar et al., 2015; Dubois et al., 2017). This program is sequential and involves four main stages: (1) initiation, (2) morphogenesis, (3) expansion and (4) senescence (Dengler and Tsukaya, 2001).

Leaf initiation originates from a pool of pluripotent stem cells located at the shoot apical meristem (SAM) (Barton, 2010). Functionally, the SAM is divided into three zones, a central zone (CZ) containing pluripotent stems cells that organize and renew the meristem, a peripheral zone (PZ) from which leaves initiate, and a rib zone (RZ) that provides cells for the stem (Aichinger et al., 2012; Tsuda and Hake, 2016). In the early stages of development, the founder cells are recruited from PZ at the site of the incipient leaf primordium. The leaf initiation starts with an auxin maximum being generated by the auxin efflux carrier PINFORMED1 (PIN1) (Reinhardt et al., 2003; Heisler et al., 2005; Johnston et al., 2015). Auxin triggers activation of the auxin-responsive transcription factor MONOPTEROS (MP; ARF5), which down-regulates the *SHOOTMERISTEMLESS* (*STM*) gene (Chung et al., 2019). STM encodes a class I KNOTTED-LIKE HOMEOBOX (KNOX1) transcription factor responsible for maintaining the stem cell fate in the SAM (Jasinski et al., 2005; Yanai et al., 2005).

The morphogenesis stage involves developmental processes in which the leaf shape develops as growth progress (Ha et al., 2007, 2010). At this stage, primordium grows predominantly in the distal direction. During this process, cells in the primordium develop a polarity gradient along the adaxial-abaxial axis (Bowman and Floyd, 2008; Qi et al., 2017). The polarity is determine by interactions between genes that specify its adaxial or abaxial identity (Bowman et al., 2002; Kidner and Timmermans, 2007). The cells identity in the adaxial domain depends on the expression of *REVOLUTA* (*REV*), *PHABULOSA* (*PHB*), and *PHAVOLUTA* (*PHV*) genes, which encode class III homeo domain-leucine zipper (HD-ZIPIII) proteins (McConnell et al., 2001; Emery et al., 2003; Caggiano et al., 2017; Yu et al., 2017). Abaxial domain identity depends on the KANADI1 (KAN1) gene expression and members of the YABBY gene family (Eshed et al., 2001; Kerstetter et al., 2001; Stahle et al., 2009; Sarojam et al., 2010; Yu et al., 2017). These two classes of genes produce signals that suppress each other's expression creating an asymmetric distribution of cells and tissue types that

determine final leaf shape (Reinhart et al., 2013; Huang et al., 2014; Xie et al., 2015).

The third stage of leaf development, the expansion, encompasses a more extended period and represents an increase in leaf surface area and volume (Pantin et al., 2012). At this stage, the expansion occurs at similar rate across the leaf, but cells at the tip of the leaf cease to expand first while the cells at the base continue the expansion until the leaf is fully expanded (Donnelly et al., 1999; Beemster et al., 2005; Fournier et al., 2005). Two classes of miRNA/transcription factors modules play dominant and antagonistic roles in sustaining cell proliferation and expansion during the expansion stage (Palatnik et al., 2003; Liu et al., 2009; Rodriguez et al., 2010; Wang et al., 2011). The module miR319, also called miRJAW in *Arabidopsis* and its target genes TEOSINTE BRANCHED1/CYCLOIDEA/PROLIFERATING CELL FACTOR (TCP) transcription factors promote the switch from cell proliferation to cell expansion by regulating the expression of miR396 (Cubas et al., 1999; Ori et al., 2007; Li et al., 2012). The activation of miR396 by TCPs transcriptionally repressed several GROWTH-REGULATING FACTORS (GRFs) genes (Liu et al., 2009; Wang et al., 2011) that formed the second module with miR396. The GRFs are a family of transcription factors that delay the transition from proliferation to expansion in leaf development by modulating the levels of cyclins (Lee et al., 2009; Debernardi et al., 2014).

Along with regulation provided by miRNA-transcription factor modules, hormonal regulation also plays a role in regulating the expansion stage. Gibberellins (GAs) and brassinosteroids (BRs) contribute to leaf growth by enhancing cell proliferation and expansion (Achard et al., 2009; Tong et al., 2014). Overexpression of GA biosynthetic enzymes or constitutive activation of GA signalling leads to larger leaves (Choe et al., 2001a). The positive effect of GAs on cell proliferation relies on the repression of cell-cycle inhibitors, such as KIP-RELATED PROTEIN 2 (KRP2) and SIAMESE (Achard et al., 2009). On the other hand, blocking GA signalling decreases leaf size (Huang et al., 1998; Achard et al., 2009).

The overexpression of *BRASSINOSTEROID INSENSITIVE1*, encoding the BR receptor, or *DWARF4,* a BR biosynthetic gene, results in larger leaves (Choe

et al., 2001b; Gonzalez et al., 2010; Zhiponova et al., 2013). Mutants deficient in BR biosynthesis or signalling display reduced leaf size and lower cyclinB (CYCB) expression, suggesting that BR controls the cell division process (Zhiponova et al., 2013). Moreover, BR signalling represses PEAPOD1 (PPD1) and PPD2, which encode transcription factors that limit the proliferation of the stem cell-like cells, called meristemoids (Gonzalez et al., 2015).

Senescence is the last stage of leaf development preceding its death (Woo et al., 2016). During senescence, leaf cells undergo significant changes in cell structure, metabolism and gene expression (Breeze et al., 2011; Woo et al., 2016; Otegui, 2018). In this stage, the chloroplast breakdown and macromolecules recycle nutrients that are supplied to nutrient sinks such as roots, young leaves and seeds (Ishida et al., 2014; He et al., 2020; Lornac et al., 2020).

These four development stages are tightly regulated at the molecular level (Li et al., 2020; Vercruysse et al., 2020). However, the final size of the leave is often adjusted based on the environmental conditions (Clauw et al., 2015; Urano et al., 2022). In general, during the early stages of leaf development, initiation and morphogenesis, leaves respond less to environmental perturbations (Zhao and Traas, 2020). At these early stages leaf primordia are well protected within the bud, and the distribution of resources within the plants, such as water and nutrients, are channelled to the young leaves, even during times of stress. As leaves undergo the expansion stage and senescence, they are more vulnerable to environmental cues (Parent et al., 2010).

1.1.2 Root growth and development

At the growing root tip, root apical meristem (RAM) contains a pool of stem cells that originates all roots tissues. In the model plant *Arabidopsis thaliana*, the RAM have five sets of stem cells (initials): vasculature initials, cortex/endodermal initials (CEI), epidermis and lateral root cap initials (EPI LRC STEM CELLS), pericycle initials and columella initials (Dolan et al., 1993; Scheres et al., 2002). These sets of cells surround the quiescent centre (QC), (Van Den Berg et al., 1997) which is essential to maintain stem cell fate through WUSCHEL-RELATED HOMEOBOX 5 (WOX5) transcription factor (Sarkar et al., 2007; Bennett et al., 2014; Forzani et al., 2014).

During root tip expansion, stem cells are maintained in the central meristem zone by cell division, while a number of cells at the distal end make their way through mitosis, enter the transition zone and subsequently extend rapidly in the elongation zone driving the root growth (Dolan et al., 1993; Heidstra and Sabatini, 2014; Di Mambro et al., 2017). This growth and development result from the coordinated action of several plant hormones. The root tip expansion starts with the polar auxin transport mediated by auxin efflux carrier PIN1 (Petrášek and Friml, 2009) from shoot to the root tip. Then, auxin is transported shootward by PIN2, establishing an auxin maxima at the QC. These auxin transport mechanisms also establish a gradient distribution of auxin in the meristem zone (Grieneisen et al., 2007; Bargmann et al., 2013; Chaiwanon and Wang, 2015). Auxin gradient regulate many key transcription factor during root growth. For example, the master regulator of root organogenesis, PLEOTHORA (PLT) transcription factor, activate cell proliferation in the root due to the auxin suppression of SHORT HYPOCOTYL 2 (SHY2) responsible for the ARFs inhibition that is necessary to activate PLT (Moubayidin et al., 2010; Salvi et al., 2020). Furthermore, auxin represses a large number of genes involved in cell elongation, which are activated by brassinesteroids (BRs) (Chaiwanon and Wang, 2015). BRs promote root cell elongation mainly through activation of BRZ1 transcription factors (Guo et al., 2013; Vragović et al., 2015).

Besides the primary root, the root system is constitute of another two different root types: lateral root and adventitious roots (Bellini et al., 2014). While the lateral root is a root that formed from a root tissue, the adventitious root originated from shoot tissue (Omary et al., 2022). These two root types share key elements of genetic and regulatory networks, however they are subject to different regulatory mechanisms. Although the transcriptions factors ARF7 and ARF19 are essential during lateral root initiation by activating the transcription factor LATERAL ORGAN BOUNDARIES DOMAIN 16 (LBD16), in adventitious root initiation WUSCHEL RELATED HOMEOBOX 11 (WOX11) transcription factor is responsible for the LBD16 activation (Liu et al., 2014).

1.2 The role of microbiota in regulating plant growth

In nature, plants are colonized by microbial communities consisting of hundreds to thousands species of bacteria, archaea, fungi, viruses, protists and

other microbial eukaryotes, collectively known as plant microbiota (Turner et al., 2013; Hacquard et al., 2017; Walters et al., 2018). Plant microbiota originates mainly from the soil, air, and via vertical transmission (transferred from parent to progeny) (Truyens et al., 2015; Wagner et al., 2016). Plant-associated microorganisms play an essential role in plant health and growth (Lebeis et al., 2015; Finkel et al., 2019). They are involved in host nutrient uptake and use (Hiruma et al., 2016; Castrillo et al., 2017), plant abiotic stress tolerance (Rolli et al., 2015; Santos-Medellín et al., 2017), and plant protection against pathogens (Vogel et al., 2021).

The plant-associated microbiota can directly or indirectly provides benefits to plant growth and health through several mechanisms (Castrillo et al., 2017; Harbort et al., 2020b; Vogel et al., 2021). The direct mechanisms are based on the production of substances that either facilitate resource acquisition or modulate plant hormone levels (Shi et al., 2010; Spaepen et al., 2014a), while the indirect mechanism involves the decrease of deleterious effects of plant-pathogens (Ritpitakphong et al., 2016; Helfrich et al., 2018).

The mechanisms of plant growth promotion driven by the microbiota effect on nutrient acquisition have been extensively studied in the case of the rhizosphere (Gouda et al., 2018; Zhang et al., 2019; Danish et al., 2020). For example, nitrogen-fixing rhizobia and mycorrhizal fungi have been extensively reported as influencing plant nutrient status by providing plants with nitrogen (N) and phosphorus (P), increasing nutrient availability, or enhancing nutrient acquisition capacity in the soil (Smith and Smith, 2011; Udvardi and Poole, 2013; Chiu and Paszkowski, 2019; Schwember et al., 2019). In addition, members of the microbiota, other than rhizobia, increase the availability and uptake of phosphorus (P), zinc (Zn), and iron (Fe) (Goteti et al., 2013; Vaid et al., 2014; Pandey and Gupta, 2020; Chen et al., 2021) by releasing phosphatase enzymes or organic chelates in the rhizosphere (Sharma et al., 2003; Richardson and Simpson, 2011; Jain et al., 2020). Hormones such as auxin and cytokinins (CKs) produced by rhizobacteria, alter root system architecture, that could indirectly enhancing nutrient acquisition by the roots (Spaepen et al., 2007, 2014b; Zamioudis et al., 2013; Bailly et al., 2014).

Furthermore, diverse members of microbiota associated with plants promote plant growth indirectly by protecting them from biotic stress (Berg; Berendsen et al., 2012; Mendes et al., 2013). The mechanisms by which plant-associated microorganisms protect against plant pathogens include competition for niches and nutrients, antibiosis, production of lytic enzymes, inhibition of pathogen virulence, and stimulation of the plant defence mechanisms known as induced systemic resistance (ISR) (Raaijmakers and Mazzola, 2012; Pieterse et al., 2014). For example, the MYB72 transcription factor that plays a role in induced systemic resistance, has been identified as crucial for plant adaptation to iron deficiency (Palmer et al., 2013; Stringlis et al., 2018; Zamioudis et al., 2014). MYB72 regulates genes responsible for the biosynthesis of coumarins, which are prominent compounds in root exudates with an important role in iron uptake and assimilation (Fourcroy et al., 2016; Harbort et al., 2020; Schmid et al., 2014).

2 Objectives

The plant microbiota is derived from the soil microbial community, which is governed by its own environmental cues (Delgado-Baquerizo et al., 2018, 2020). Correlations with soil microbial diversity, and by derivation, with plant microbiota composition and diversity, were observed for soil environment factors, such as pH (Lauber et al., 2009; Fierer et al., 2012), water content (Santos-Medellín et al., 2017), and nutrient concentrations (Leff et al., 2015). Emerging evidence suggests that soil microbiota play an essential role in plant growth under environmental changes. For example, Arabidopsis plants grown under variable soil phosphorus (P) conditions demonstrate shifts in the bacterial composition that affect their rosette size (Finkel et al., 2019) and the bacterial genus *Variovorax* is necessary to maintain the root growth (Finkel et al., 2020).

Given the fact that plants assemble distinct microbial communities in roots and leaves (Bai et al., 2015), we hypothesized that root and individual leaves within a plant represent differential ecological niches that recruit distinctive bacteria-resident communities in response to different environmental stressors.

To test the defined hypothesis, we built a generalized framework with the aim:

- To assess whether mineral content and bacterial composition in individual leaves could explain the variations in leaf development observed in the plant response to different soil properties.

- To investigated whether the organ response is similar or varies between leaf developmental stages, independently of variations in nutrients and microbiota at the soil level.

3 Materials and Methods

3.1 Soil variability effect on maize ionome and microbiome

3.1.1 Soil collection

For the soil experiments, we used a collection of two arable soils and a natural soil from three different geographical locations. Arable soils were collected from the INIDA station, São Domingos, Cabo Verde, a semi-arid region (331 mm of accumulated rainfall) located in the central area of Santiago island (15º1'7.6728''N, 23º32'54.3372''W) and from the INIDA station, Tarrafal, Cabo Verde, an arid region (196 mm of accumulated rainfall) located in the northern coastal area of Santiago island (15º15'17.5468''N, 23º44'38.9256''W). The natural soil, free of pesticide and fertiliser, was collected from a farm located at Sutton Bonington Campus, University of Nottingham, UK (+52° 49′ 59.75″N, −1° 14′ 56.62″W). Before soil collection, all tools were washed with water and disinfected with 70 % ethanol. Approximately the first 5-10 cm of the soil containing the local vegetation, was discarded and the collected soil was stored in clean plastic boxes at 4 °C until use.

3.1.2 Soil preparation

Collected soils were dried in cleaned plastic trays at room temperature for one week and then sifted using ethanol disinfected 2 mm sieve. Soils were mixed with autoclaved pavior sand in a proportion of 2:1 (v/v) to increase the soil drainage and decrease soil compaction. Sterile pots, with a square of sterilised Miracloth (Millipore) at the bottom, were weighted and filled with 300 g of each soil mixture and used to grow *Zea mays* plants.

3.1.3 Plant growth conditions. Nutrient effect

To determine the soil effect on leaf ionome and microbiome, we analysed a collection of *Zea mays* genotypes (B73, Matuba, CVSt and Zm523) that represent different levels of adaptation to nutrient and water content in soils (Chen et al., 2012; Thierfelder et al., 2016).

All seeds were surface-sterilized with 70 % bleach, 0.2 % Tween-20 for 8 min, followed by three rinses with sterile distilled water to eliminate any seed-

borne microbes on the seed surface. Before sowing, seeds were placed in 9 cm Petri dishes with 10 mL of sterile water and incubated at 30ºC in the dark overnight to promote germination. Maize seeds were then sown in the soil mixtures prepared as described above using sterile tweezers, and as controls, we used unplanted pots ("bulk soil").

Pots were randomised using a true random generator (random.org), and trays were reshuffled every day in the growth chamber. All pots, including controls, were daily watered with autoclaved Milli-Q water (18.2 MΩ cm; Merck Millipore) using a pump-action pressure spray bottle (Hozelock, Ltd, England).

Plants were grown in a growth chamber under 16-h light/8-h dark at 26 ºC day/24 ºC night, 500 µE m^{-2} s^{-1} photosynthetically active radiation regime. We repeated this experiment twice using three replicas per treatment.

3.2 Characterisation of plant phenotypes

3.2.1 Quantification of leaf length

At harvest time, the image of maize shoot was manually acquired using an EOS 4000D DSLR camera (Canon) with an 18-55 mm lens in the automatic mode. The flash function was kept off, and images were stored in JPEG format. Individual leaf length was determined from images using the Measure function in ImageJ software (Schneider et al., 2012). After Set scale in cm in each image, leaf length was determined by drawing a line from the leaf base to the leaf tip using the "freehand" function in lmageJ and measuring it using the Measure function.

3.2.2 Determination of individual leaf and root biomass

To determine the individual leaf dry weight, leaves were collected individually and dried in an oven at 70 ºC for three days. Individual leaves were weighted using a Metler four-decimal analytical scale. In the root case, the total root system was collected and rinsed with water to remove the soil particles attached. Cleaned roots were lyophilized in an Alpha 2-4 LD freeze dry system and then weighted in Metler four-decimal analytical scale.

3.2.3 Analysis of leaf mineral elemental profile

The elemental profiles of individual leaves were measured using Inductively Coupled Plasma Mass Spectrometry (ICP-MS). Individual leaves were collected from the plant at the V4-developmental stage (leaf number 4 fully expanded with the collar formed). The leaf material was washed three times with 18.2 MΩcm Milli-Q water (Merck Millipore) and cut into small pieces using a clean ceramic scalpel. Representative samples containing fragments from the different regions of the leaf were collected in a sterile 1.5-mL Eppendorf tube and stored at 4 ºC until further use. The leaf samples were placed in weighted Pyrex digestion tubes and dried at 88 ºC for 20-h. After cooling, leaf samples were weighted on Mettler five-decimal analytical scale, and 1-3 mL (depending on the sample dry weight) of the concentrated trace metal grade nitric acid Primar Plus (Fisher Chemicals) was added to each tube. Prior to the digestion, 20 µg/L of Indium (In) was added to the nitric acid as an internal standard to assess putative errors in dilution, variations in sample introduction and plasma stability in the ICP-MS instrument. The samples were then digested in DigiPREP MS dry block heaters (SCP Science; QMX Laboratories) for 4-h at 115 ˚C. After cooling down, the digests were diluted to 10-30 mL (depending on the volume of the nitric acid added) with 18.2 MΩcm Milli-Q Direct water and elemental analysis was performed using an ICP-MS, PerkinElmer NexION 2000 equipped with Elemental Scientific Inc 4DXX FAST Dual Rinse autosampler, FAST valve and peristaltic pump. The instrument was fitted with a PFA-ST3 MicroFlow nebulizer, baffled cyclonic C3 high sensitivity glass spray chamber cooled to 2 ºC with PC3X Peltier heated/cooled inlet system, 2.0 mm i.d. quartz injector torch and a set of nickel cones. Twenty-four elements were monitored including following stable isotopes: ^{7}Li, ^{11}B, ^{23}Na, ^{24}Mg, ^{31}P, ^{34}S, ^{39}K, ^{43}Ca, ^{48}Ti, ^{52}Cr, ^{55}Mn, ^{56}Fe, ^{59}Co, ^{60}Ni, ^{63}Cu, ^{66}Zn, ^{75}As, ^{82}Se, ^{85}Rb, ^{88}Sr, ^{98}Mo, ^{111}Cd, ^{208}Pb and ^{115}In. Helium was used as a collision gas in Kinetic Energy Discrimination mode (KED) at a flow rate of 4.5 mL/min while measuring Na, Mg, P, S, K, Ca, Ti, Cr, Mn, Fe, Ni, Cu, Zn, As, Se and Pb to exclude possible polyatomic interferences.

The remaining elements were measured in the standard mode. The instrument Syngistix™ software for ICP-MS v.2.3 (Perkin Elmer) automatically corrected any isobaric interferences. The ICP-MS measurements were

performed in peak hopping scan mode with dwell times ranging from 25 to 50 ms depending on the element, 20 sweeps per reading and three replicates. The ICP-MS conditions were as follow: RF power – 1600 Watts, auxiliary gas flow rate 1.20 L/min. Torch alignment, nebuliser gas flow and quadrupole ion deflector (QID) voltages (in standard and KED mode) were optimized before analysis for highest intensities and lowest interferences (oxides and doubly charged ions levels lower than 2.5 %) with NexION Setup Solution containing 1 µg/L of Be, Ce, Fe, ln, Li, Mg, Pb and U in 1 % nitric acid using a standard built-in software procedure. To correct for variation between and within ICP-MS analysis runs, liquid reference material was prepared using pooled digested samples and run after the instrument calibration and then after every nine samples in all ICP-MS sample sets. Equipment calibration was performed at the beginning of each analytical run using seven multi-element calibration standards (containing 2 µg/L In internal standard) prepared by diluting 1000 mg/L single element standards solutions (Inorganic Ventures; Essex Scientific Laboratory Supplies Ltd) with 10 % nitric acid. As a calibration blank, 10 % nitric acid containing 2 µg/L In internal standard was used, and it was run throughout the analysis. Sample concentrations were calculated using the external calibration method within the instrument software. Further data processing, including calculation of final elements concentrations, was performed in Microsoft Excel.

3.3 Analysis of soil mineral elemental profile

For the soil mineral elemental analysis, soil samples were harvested from the individual pots and placed in 50 ml Falcon tubes. The soil samples were first dried using a plastic weighing boat in the fume hood for approximately 72h at room temperature. Five grams of soil was then weighted in 50 ml Falcon tubes with a four-decimal scale, and digested with 20 mL of 1 M NH_4HCO_3, 5 mM diamine-triamine-penta-acetic acid (DTPA), and 5 mL 18.2 MΩcm Milli-Q Direct water (Merck Millipore), 1h at 150 rpm in a rotary shaker (adapted from (Soltanpour and Schwab, 1977). Each sample was gravity filtered through a quantitative filter paper (Whatman 42- WHA1442070) until obtaining approximately 5 mL of filtrate. 0.5mL of the filtrates were open-air digested in Pyrex tubes using 1 mL of concentrated trace metal grade nitric acid Primar Plus (Fisher Chemicals) spiked with 20 µg/L indium internal standard for 4-h at 115 ºC

in dry block heater (DigiPREP MS, SCP Science; QMX Laboratories, Essex, UK). Each sample was then diluted up to 10 mL with 18.2 MΩcm Milli-Q Direct water. The elemental analysis was performed using PerkinElmer NexION 2000 ICP-MS equipped with Elemental Scientific Inc. autosampler in the collision mode (He) as described for leaf samples. To correct for variation between and within ICP-MS analysis runs, liquid reference material was prepared using pooled digested samples and run in the same manner as leaf samples. Sample concentrations were calculated using the external calibration method within the instrument software. Further data processing to obtain the final concentration of the elements was performed in Microsoft Excel and included correction of the drift, subtraction of the blank concentration, multiplication by the dilution factor and normalization to the soil dry weight.

3.4 Ionome analysis

In conjunction, for both leaves and soil elemental profiles, we created a matrix (samples x ion) in which each cell was filled with the calculated element concentration in a given sample. Afterwards, we applied a z-score transformation of each ion across the samples in the matrix. Next, we applied a principal component analysis (PCA) using the Euclidean distance between samples and the z-score matrix as input to compare the elemental profiles of leaves and soil. Additionally, we estimated the variance explain by soil origin, fractions and leaf number by performing PERMANOVA via the function adonis from the vegan v2-5.5 R package (Oksanen, 2007).

For the natural soil characterization experiment, we compared the concentration of each ion in the three soils against each other by fitting a linear model with the following design:

$$\text{Ion concentration} \sim \text{Soil}$$

After fitting the model, we applied the pairwise comparisons. Further, we used the false discovery rate (FDR) approach to adjust the p-values obtained from the pairwise comparisons. An ion was considered significant for each comparison if it had a p-value < 0.05. The enrichment profiles of each ion across the shoot and soil fractions were visualized using a heatmap created by the ggplot2 v.3.2.1 (Wickham, 2016), R package.

For the enrichment in the single-leaves experiment, we used the same approach described above with a different linear model design:

Ion concentration ~ Number of leaf (NumLeaf) + Soil

3.5 Analysis of microbiome composition

3.5.1 DNA extraction

Microbiota composition was determined in individual leaves, roots and soil samples from plants grown using the three soils described in material and methods 2.1. At the harvesting time, individual leaves were cut into small pieces using a sterile scalpel. A representative sample containing leaf fragments from the different regions of the leaf was collected in a sterile 2-mL Eppendorf tube. Leaf samples were rinsed three times with sterile distilled water to remove weakly associated microbes and soil particles. The whole root system was also collected and rinsed three times with sterile distilled water in 500 mL glass bottles. Soil samples were collected in 50 mL falcon tubes containing sterile distilled water and then filtered using sterile 100 µm nylon mesh cell strainers (Fisherbrand^{TM}, Thermo Fisher Scientific Inc.) to remove plant debris and big soil particles. Then, soil samples were centrifuged at room temperature for 20 min at max speed in an Eppendorf 5810R centrifuge, and the supernatant was discarded. The pellet was dissolved in 1 mL of sterile water, and the resulting suspensions were transferred to sterile 1.5-mL Eppendorf tubes. Samples were centrifuged again at high speed in a benchtop centrifuge, and the supernatants were discarded. All samples were stored at -80 ºC until use.

Before DNA extraction, leaf and roots samples were lyophilized using an Alpha 2-4 LD freeze dry system. Individual root systems were cut into small pieces using flame-sterilized scissors, and a representative root sample was transferred to 2-mL Eppendorf tubes. Leaf and roots samples were pulverised using a Tissue Lyser II (Qiagen) with the following conditions: 4 cycles of 60 seconds at the frequency of 30 s^{-1}. The DNA extraction was carried out using 96-well-format MoBio PowerSoil Kit (MOBIO Laboratories; Qiagen) following the manufacturer's instruction. Before starting the extraction, leaf, root and soil samples were manually randomised by shaken them several times in a plastic bag. Samples were taken individually from the bag and loaded into the DNA

extraction plates. This random distribution was maintained throughout library preparation and sequencing.

3.5.2 16S rRNA amplification and sequencing

For the 16S rRNA sequencing, the V3-V4 region of the bacterial 16S rRNA gene was amplified using the primers 338F (5′-ACTCCTACGGGAGGCAGCA-3′) and 806R (5′-GGACTACHVGGGTWTCTAAT-3′). Each sample was amplified in triplicate, and the PCR reactions were performed using three sets of unique primers combinations per plate. The following conditions were used for PCR amplification: 5 µL Kapa Enhancer, 5 µL Kapa Buffer A, 1.25 µL of 5µM 338F, 1.25 µL of 5µM 806R, 0.375 µL mixed plastid and mitochondrial rRNA gene-blocking peptide nucleic acids (PNAs; 1:1 mix of 100 µM plastid PNA and 100 µM mitochondrial PNA), 0.5 µL Kapa dNTPs, 0.2 µL Kapa Robust Taq, 8 µL dH2O and 8 µL DNA; temperature cycling: 95 °C for 1 min, 24 cycles of 95 °C for 15 s, 78 °C (PNA) for 10 s, 50 °C for 30 s, 72 °C for 30 s and 4 °C until use. PCR products of triplicate were combined and purified using AMPure XP magnetic beads (Beckman Coulter) to remove primer dimers. 10 µL of purified DNA was subjected to a second PCR using the following conditions: 12 µL Kapa HiFi Readymix, 0.375 µL mixed (1:1) of 100 µM pPNA and 100 µM mPNA; 2.5 µL of 5 µM index primers; temperature cycling: 95 ºC for 1 min, 9 cycles of 95 ºC for 15 s, 78 ºC for 10 s, 60 ºC for 30 s, 72 ºC for 35 s and 4 °C until use. Subsequently, amplicons were pooled together in equal amounts and then diluted to 10 pM for sequencing. Sequencing was performed on an Illumina MiSeq instrument using a 600-cycle V3 chemistry kit in the DeepSeq facility at the University of Nottingham. DNA sequence data, the abundance matrix, metadata and taxonomy will be available upon publication.

3.5.3 16S rRNA amplicon sequence data processing

For the 16S rRNA analysis, sequences data were processed with cutadapt (Martin, 2011), DADA2 and R packages. Raw reads were demultiplexed and trimmed with cutadapt. The resulting sequences were then denoised and collapsed into amplicon sequence variants (ASVs), using DADA2 v.1.10.1 (Callahan et al., 2016). Briefly, the paired reads were filtered by removing sequences containing uncalled bases, truncating reads after bases with a quality

score of 2 and reads with no more than 3 expected errors using the FilterAndTrim function. We then learn the error for the forward and reverse reads separately with the learnErrors function. These error rates were then used to infer amplicon sequence variants (ASVs) with the function dada on the reverse and forward reads individually. After, we merge the forward and reverse sequence with the mergePairs function. The merged ASVs were used to build an ASV sequencing table using the makeSequenceTable function. Then, we removed chimeras from the sequence table with the removeBimeraDenova function. The resulting ASVs were mapped to SILVA 132 database (Quast et al., 2013). We filtered ASVs that were assigned to chloroplast, mitochondria, oomycete, archaea or did not have a known kingdom assignment. After the filtering, the remaining ASVs, with more than 1000 reads per sample, were used to create the raw count abundance tables. The resulting abundance tables were processed and analysed with functions from the ohchibi package (https://github.com/isaisg/ohchibi).

3.5.4 16S rRNA amplicon sequence analysis

To compare alpha diversity across soils, roots, and individual leaves, we calculated the Shannon diversity index using the diversity function from the vegan package v2.5-5 (Oksanen, 2007). We used ANOVA to test for differences in alpha diversity between the different fractions. Beta diversity analyses (Principal coordinate analysis, Pco and canonical analysis of principal coordinates, CAP) were based on Bray-Curtis dissimilarity matrices calculated from the rarefied abundance tables. Additionally, we estimated the variance explain by soil origin, fractions and leaf number by performing PERMANOVA via the function adonis from the vegan v2-5.5 R package (Oksanen, 2007). We applied PCo using the function prcomp in R.

The relative abundance of bacterial phyla was depicted using a stacked bar representation encoded in the function chibi.phylogram from the ohchibi package (https://github.com/isaisg/ohchibi).

For the enrichment profile in the natural soil characterization experiment, we used the R package DESeq2 v.1.24.0 (Love et al., 2014) to compute the soil origin-specific enrichment profiles. For each phylum in the abundance tables, we estimated its difference in abundance with the three different soils (Tarrafal, São

Domingos and Sutton Bonington) by fitting a Generalized Linear Model (GLM) with the following design:

$$Abundance \sim Soil$$

From the fitted model, we extracted the following comparisons: Tarrafal vs São Domingos, Tarrafal vs Sutton Bonington and São Domingos vs Sutton Bonington. A phylum was considered statistically significant if it had a p-value < 0.05. We visualized the results for the GLM using a heat map. The rows in the heat map were ordered according to the dendrogram obtained from the phyla analysis. The heat map was coloured based on the $\log_2$-transformed fold change output by the GLM. The significant comparisons (p-value < 0.05) were highlighted with black framing.

4 Results and Discussion

4.1 Soils from Cabo Verde and UK represent different levels of variability in mineral content and bacterial composition

Plant growth largely depends on soil water content, the combination and concentration of mineral nutrient availability in soil, and soil microbiota composition (Salas-González et al., 2021). To demonstrate the soil effect on plant growth, we selected three different soils, and we first determined the mineral content profiles and the bacterial composition of each soil. Two arable soils with an irregular rainy season and few heavy rains were selected from Santiago Island (Cabo Verde) (Baptista et al., 2015) to compare with rich soil (free of pesticides and fertilizers) with a history of high precipitation exposure, from Sutton Bonington (Nottingham, UK). Six replicas of each soil were analysed in two independent experiments to determine nutrient content and profiles of bacterial communities.

We examined differences in soil mineral content in the different soils using Inductively Coupled Plasma Mass Spectrometry (ICP-MS). Principal component analysis (PCA) of the mineral nutrient profiles showed that all the soils are different in terms of their mineral nutrient composition (adonis: degrees of freedom (df) = 2; coefficient of determination (R^2) = 0.84; $P<0.001$) (Figure 1A). To further explore the variation of different elements per soil, we calculated pairwise comparisons in soil mineral content across all soils. We identified four well-defined groups of mineral nutrients that appeared in either enriched or depleted concentrations across the different soils (Figure 1B). Group 1(G1) contained Zn, U, Se, Pb, P, Mo, Mn, Fe, Cr, Co, Cd, As, Al and Ag were predominantly enriched in Sutton Bonington samples, which suggest that this clade is driving the differences between the soils from the two countries. Group 2 (G2), containing Rb, K, and Ba, showed an enrichment pattern in Tarrafal soil. Group 3 (G3) containing V, Sr, S, Ni, Mg, Cu, Ca, and B showed an enrichment pattern in São Domingos soil, whereas group 4 (G4) reflected an enrichment pattern in Ti and Na in Cabo Verde soils (both Tarrafal and São Domingos).

We then investigated the bacterial composition in the three soils. Total DNA was extracted from soils, and the 16S rRNA (V3-V4) regions were amplified and

sequenced using Illumina platform. Sequences were collapsed into amplicon sequence variants (ASVs) and we measured the α-diversity (within-sample diversity) and β-diversity (between-sample diversity) across the different soils. We estimated α-diversity across soils by calculating the Shannon diversity index. São Domingos and Sutton Bonington showed quantitatively similar index and higher than Tarrafal soil, indicating that microbial diversity in these two soils was higher than Tarrafal (Figure 1C). As we expected, we found that bacterial communities' composition differs among soils. Principal coordinates analysis (PCo) showed that the different soils carried different bacterial communities (Figure 1D). The primary axis (PCo1) of variation distinguished the Cabo Verde soil microbiomes from the one of Sutton Bonington. In contrast, the secondary axis (PCo2) of variation separated between the soils collected in Cabo Verde (Tarrafal and São Domingos). Then, we investigated the abundance patterns of bacterial phyla found in each soil. The general taxonomic patterns in each soil are driven mainly by differences in the abundances of taxonomic groups. The Actinobacteria, Chloroflexi, and Proteobacteria phyla were generally abundant in the three soils, whereas Bacteroidetes, Planctomycetes and Acidobacteria showed an opposite pattern (Figure 1E).

To study which phyla are enriched in the different soils, we utilized a generalized linear model (GLM). We found that Actinobacteria, Planctomycetes, and Firmicutes phyla were significantly enriched in Cabo Verde soils (Figure 1F). In contrast, Latescibacteria, Verrucomicrobia, and Nitrospirae showed significant enrichment in Sutton Bonington soil. Whereas, Proteobacteria and Gemmatimonadetes showed an enrichment pattern in Tarrafal soil samples, suggesting that these phyla drive the difference between Cabo Verde soils. Taken together, these results demonstrate that our soils selection represent different level of variability in mineral content and bacterial composition.

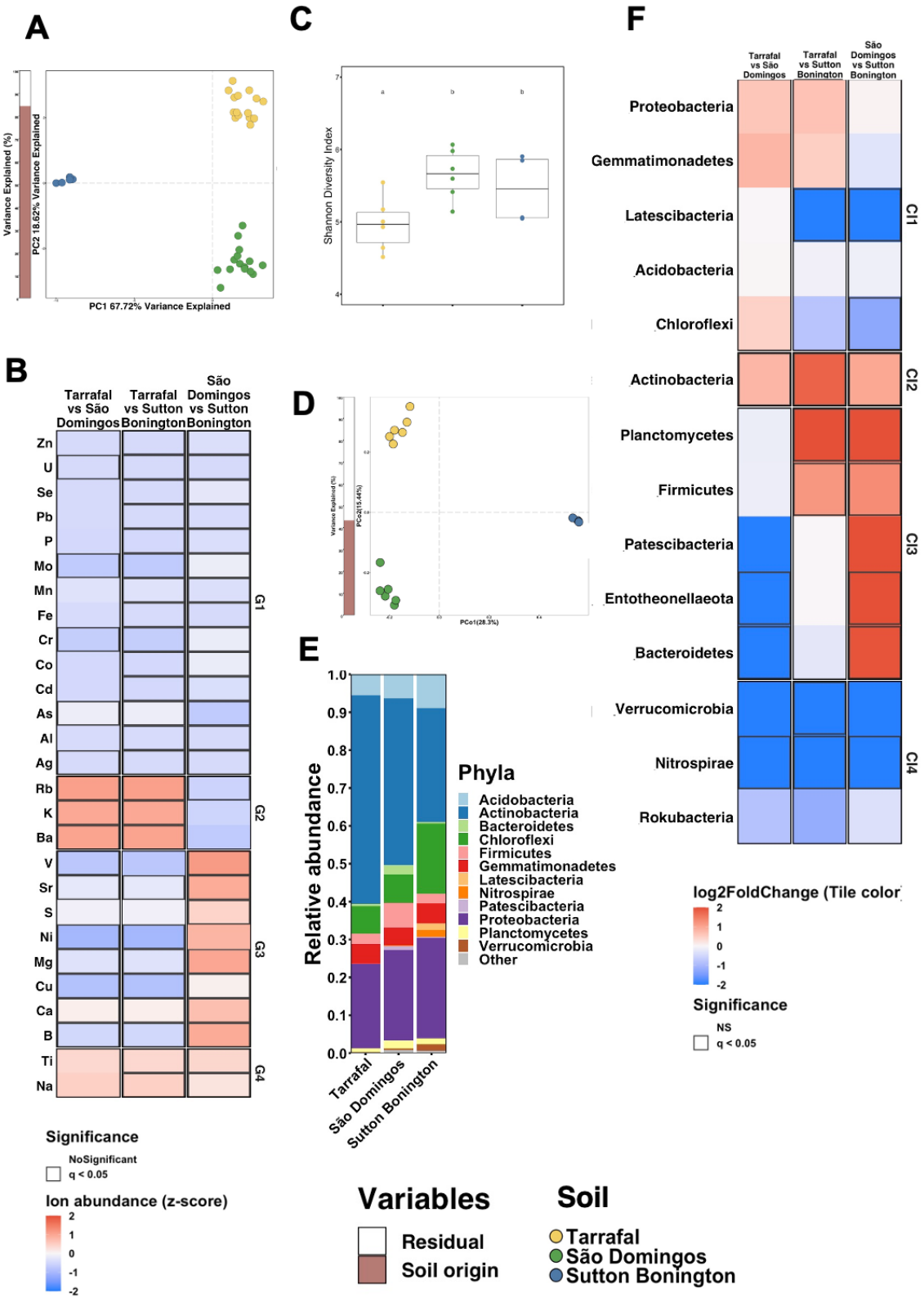

Figure 1: The selected soils differ strongly in mineral content and microbiome composition. (A) Principal component analysis (PCA) based on Euclidean distance between mineral content across soils. The bar graph to the left of the PCA represents the percentage of variance explained by statistically significant ($p < 0.05$) variables in a PERMANOVA model **(B)**

Enrichment pattern of mineral nutrient concentrations in the different soils. Each column in the heat maps represents a specific contrast in the enrichment model. The heat maps are coloured based on z-score. Positive z-score (coloured in red gradient) represent enrichments on the left side of the name of the contrast (e.g. Tarrafal vs São Domingos, enriched in Tarrafal comparing to São Domingos). In contrast, a negative z-score (coloured in blue) represent enrichments on the right side of the name of the contrast (e.g. Tarrafal vs São Domingos, enrichment in São Domingos in comparison to Tarrafal). Significant comparisons between each soil are outlined in black ($q < 0.05$). **(C)** Bacterial alpha diversity estimated using the Shannon Diversity Index. Letters represent *post hoc* test results, based on ANOVA model. **(D)** PCo based on Bray-Curtis dissimilarities between bacterial communities across soils. The bar graph to the left of the PCo depicts the percentage of variance explained by statistically significance ($p < 0.05$) variables in a PERMANOVA model. **(E)** Relative abundance profiles of the rare bacterial phyla across the three soils. **(F)** Enrichment pattern of bacterial communities in the different soil. Each row along the different panels represents a unique phylum identified in the soils. Each column in the heat maps represents a specific contrast in the enrichment model. The heat maps are coloured based on $\log_2$ fold changes derived from fitted GLM. Positive fold changes (coloured in red gradient) represent enrichments on the left side of the name of the contrast (e.g. Tarrafal vs São Domingos, enriched in Tarrafal as compared to São Domingos), whereas negative fold changes (coloured in blue) represent enrichments on the right side of the name of the contrast (e.g. Tarrafal vs São Domingos, enrichment in São Domingos in comparison to Tarrafal). Significant comparisons are outlined in black ($q < 0.05$). Principal component analysis; PCo, Principal coordinate analysis; PERMANOVA, Permutational Multivariate Analysis of variance; GLM, generalized linear model.

4.2 Roots and leaves growth respond differentially to soil mineral content

To assess the effect of different soils on plant growth, we grew four maize genotypes that represent different levels of adaptation to soil nutrient and water content (Chen et al., 2012; Thierfelder et al., 2016) in the three soils characterised in this work.

For the analysis, we harvested the plants when they reached V4 developmental stage (approximately 15 days) and we then quantified plant phenotypes such as root and shoot biomass, individual leaf biomass and length as proxies for plant growth (Figure 2). We observed genotype-specific differences in root dry weight (ANOVA, $P < 0.001$) but not soil-specific differences (ANOVA, $P=0.3212$) (Figure 2A-B). The genotypes B73 and Matuba showed the lowest root dry weight. While CVSt and Zm523 genotype showed the highest root dry weight (Figure 2A, ANOVA followed by *post hoc* Tukey's HSD). By averaging the

genotypes and analysing the root dry weight per soil, we found no significant effect of the soil on root biomass. These results indicate that the root biomass is not affected by the variability in soil mineral content or microbiome. By contrast, we found soil-specific differences in shoot dry weight (ANOVA, $P < 0.01$) (Figure 2D) but not genotype-specific differences (ANOVA, $P=0.434$) (Figure 2C). Analysis of plants grown in the two Cabo Verde soils (Tarrafal and São Domingos), showed Tarrafal with a significant difference in shoot dry weight as compared to plants grown in São Domingos soil (Figure 2D, ANOVA followed by *post hoc* Tukey's HSD), whereas, the shoot dry weight of plants grown in Sutton Bonington was similar to the shoot dry weight of plants grown in both soils from Cabo Verde (Figure 2D, ANOVA followed by *post hoc* Tukey's HSD). These findings indicate that root response to soil variability is buffered by genotypes while leaf growth is affected by soil natural variability.

To further understand shoot growth in response to the different soils, we studied individual leaf dry weight and length. We found that in all 3 soils, leaf dry weight and length was quantitatively similar in a subset of leaves (L1, L2 and L6; numbers refer to the positions of leaves according to their order of appearance) and L3 to L5 was more extensively affected by soil mineral content and microbiome variability (Figure 2E-F, ANOVA followed by *post hoc* Tukey's HSD). This finding indicates that individual leaves differentially integrate soil effect in maize.

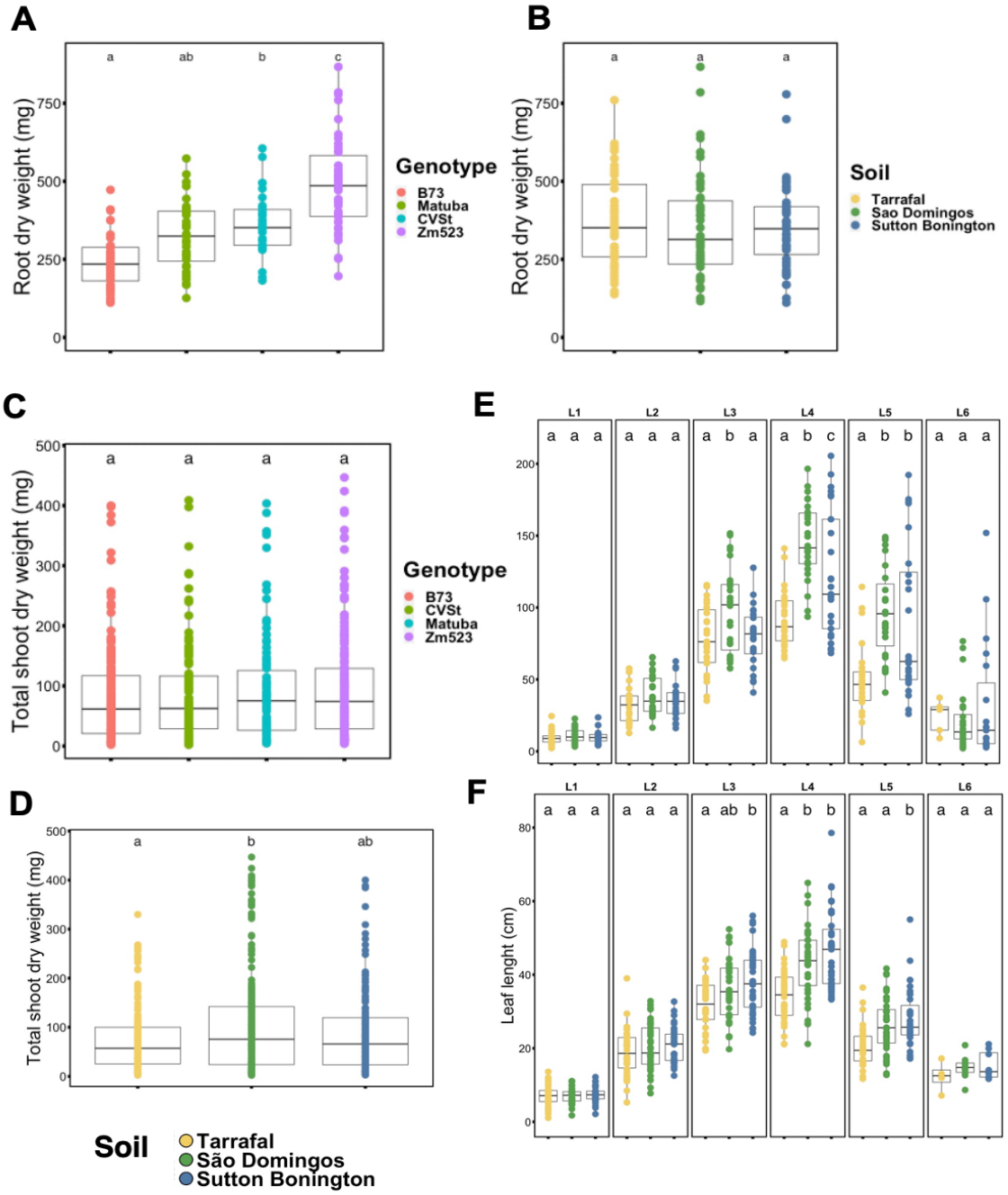

Figure 2: Leaf growth differently responds to soil natural variability. (A and **B)** Root dry weight (in mg) of four-week-old *Zea mays* grown in pots with the 3 different soils. Three independent biological replicates (n = 150 plants). **(C** and **D)** Shoot dry weight (in mg) of four-week-old *Zea mays* grown in pots with the 3 different soils. Two independent biological replicates (n = 76 plants). **(E)** Individual leaf biomass (in mg) in pots with the 3 different soils**.** Two independent biological replicates (n = 474 leaves). **(F)** Individual leaf lenght (in cm) of four-week-old *Zea mays* grown in the 3 different soils. Three independent biological replicates (n = 647 leaves). For all plots, letters indicate statistical significance corresponding to ANOVA

with Tukey's HSD *post hoc* test (α = 0.05). In all box plots, the centre line represents the median, box edges show the 25th and 75th percentiles, and whiskers extent to 1.5x the interquantile range (IQR).

4.3 Leaf age drives the variation in leaf mineral nutrient composition

To understand the factors that affect leave growth, we investigated the mineral nutrient and trace element composition of the leaves, the ionome (Salt et al., 2008) using the same maize genotypes and soils described above. The analysis of ionome in single leaves based on average Euclidean distance across replicates, revealed that ionome in leaf were separated by leaf age and soil origin (Figure 3A-B). PERMANOVA indicated that the factor leaf age (Leaf number) explains the variation in leaf ionome composition (Adonis: df = 5; R^2 = 0.24; P<0.01) than maize genotypes (adonis: df = 3, R^2 = 0.02, P<0.01) and soil origin (Adonis: df = 2, R^2 = 0.15, P<0.01) (Figure 3B). To identify the ionome signature in each leaf, we calculate pairwise correlations in ionome content across all samples. We identified eight well-defined clusters of mineral nutrients with concentrations that are enriched and depleted across individual leaves (Figure 3C). The most mobile elements in plants, K and P (Taiz et al., 2015) formed a distinct cluster (Cl1 and Cl8) with a gradient increase of concentrations as the leaf transition from L1 to L6. Interestingly, Pb, Zn, and Ni (Cl2) showed a unique pattern where the concentrations between leaves changed according to the soil used to growth the plants. Cluster 3 (Cl3) and Cluster 6 (Cl6) were composed of elements that were mainly enriched in L1 (S, B, Li, Co, Cr) and elements that were enriched in L1 and L2 (Ti, Mg, Ca, Mo), respectively, in all soils, whereas, Fe, Mn, Cd, As, and Cu were enriched in the same subset of leaves mainly in Sutton Bonington soil (Figure 3C). These data suggest that each leaf has a unique mineral element signature that depends to some extent on individual soil characteristics. This effect suggests that individual leaves in the plant may represent different ecological niches for the bacterial communities.

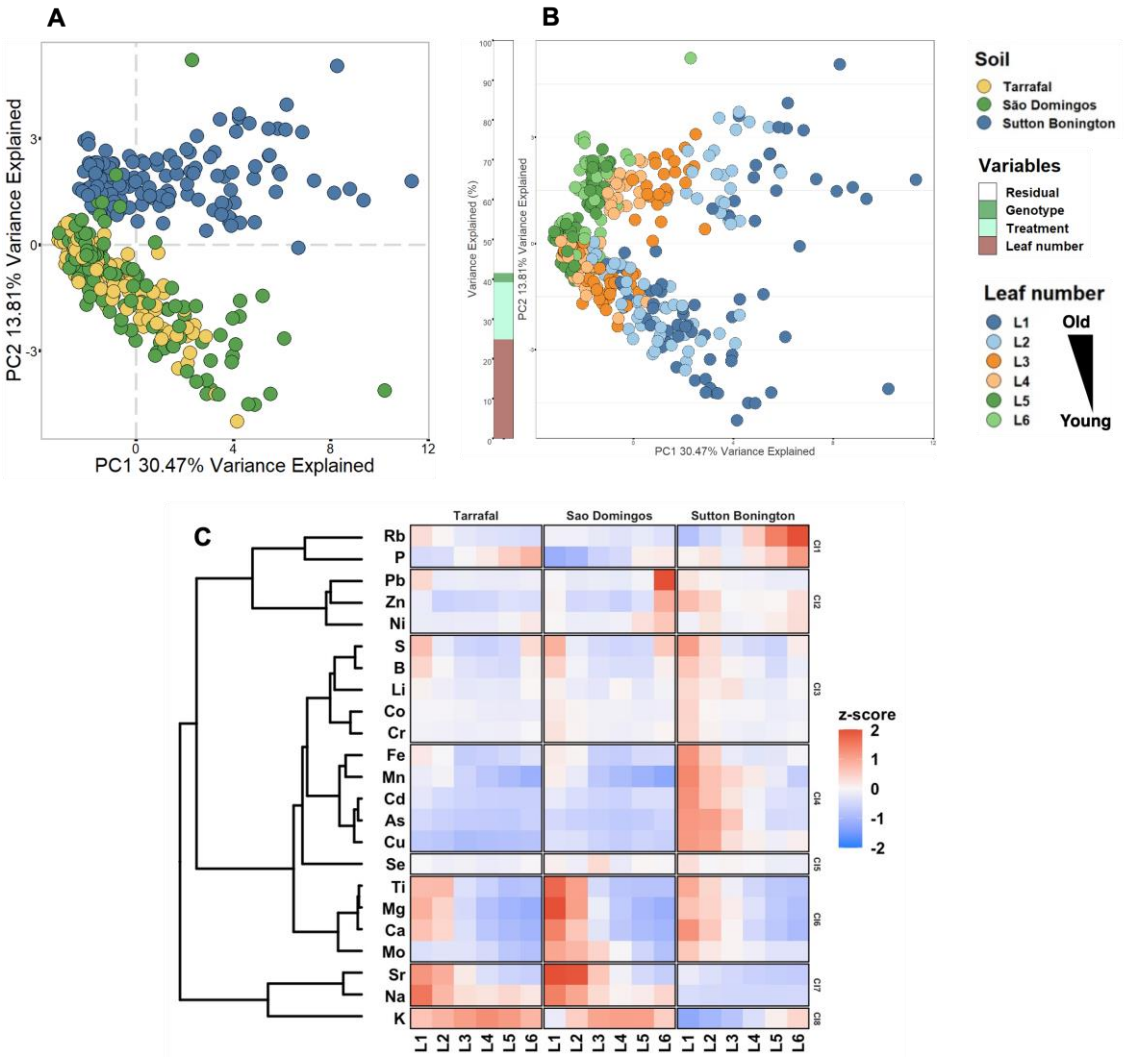

Figure 3: Leaf age effects on maize shoot ionome. (A) and (**B)** PCA analysis based on Euclidean distance of leaf mineral nutrient composition (ionome) showing the ionomic profiles of maize genotypes growing in the three soils. **(B)** The bar graph to the left of the PCA represents the percentage of variance explained by statistically significance (P<0.05) variables in a PERMANOVA model. Different colours show the leaf mineral profile in each soil **(A)** and in each leaf (**B). (C)** Heatmap showing mineral nutrient concentrations in individual leaves. The heat maps are coloured based on z-score.

4.4 Different leaves assemble different bacterial communities

To explore whether an individual leaf is able to assemble a distinct microbiome, we compared the composition of leaf-associated bacterial communities in individual leaves in 4 maize genotypes grown in pots filled with each of the three soils described above. For each genotype, we harvested soil, roots and individual leaves when the plants reached the V4 developmental stage.

We also harvested soils from unplanted pots from each soil that we used as controls. Next, we generated a bacterial community profile for each sample via PCR amplification of the 16S ribosomal RNA (rRNA) gene. We obtained 10,357,079 sequences from 514 samples. We found that alpha diversity decreased from soil to the root and shoot fractions in the three soils used in this work (Figure 4A), however diversity at shoot level was higher than at roots. Compared to *Arabidopsis*, a dicot, that shows a higher microbial diversity in root than shoot (Castrillo et al., 2017; Finkel et al., 2019), this result suggests that: (1) in monocot (maize) there is not only a different recruitment pattern of microbial communities, but also a different abundance of these communities; (2) by analysing single-leaf microbial composition we can recover a higher number of species per sample. However, further studies are needed in order to define this pattern in dicot and monocot.

Next, we explore the community composition for each fraction soil, root and shoot. We found that roots and shoots harbour bacterial communities distinct from the surrounding soil community and from each other (Figure 4B). To further explore single leaf bacterial communities, we analysed the microbial diversity and composition in individual leaves. We found that L1, L2, and L6 sustained a lower bacterial alpha diversity in Sutton Bonington soil compared to Tarrafal and to São Domingos and a higher alpha diversity for L3 to L5 (Figure 4C). Interestingly, the beta diversity analysis showed that each leaf assembles a different composition of bacterial community (Figure 4D). CAP analysis based on Bray-Curtis distances revealed significant differences in bacteria composition according to leaf number, which separated along the first coordinate axis (Figure 4D). These differences are robust across the three different soils, suggesting divergence in bacterial community in individual leaves. Finally, to explore leaf-specificity in the plant microbiome composition, we compared soil, root, and single leaves at the phyla levels. In all 3 soils, the relative abundance of Actinobacteria and Proteobacteria phyla was higher in soil and roots compared to leaves (Figure 5)., while the Firmicutes phylum was present at higher relative abundance in leaves as compared to root and soil. Our results demonstrate that maize individual leaves harbour a different microbiota community.

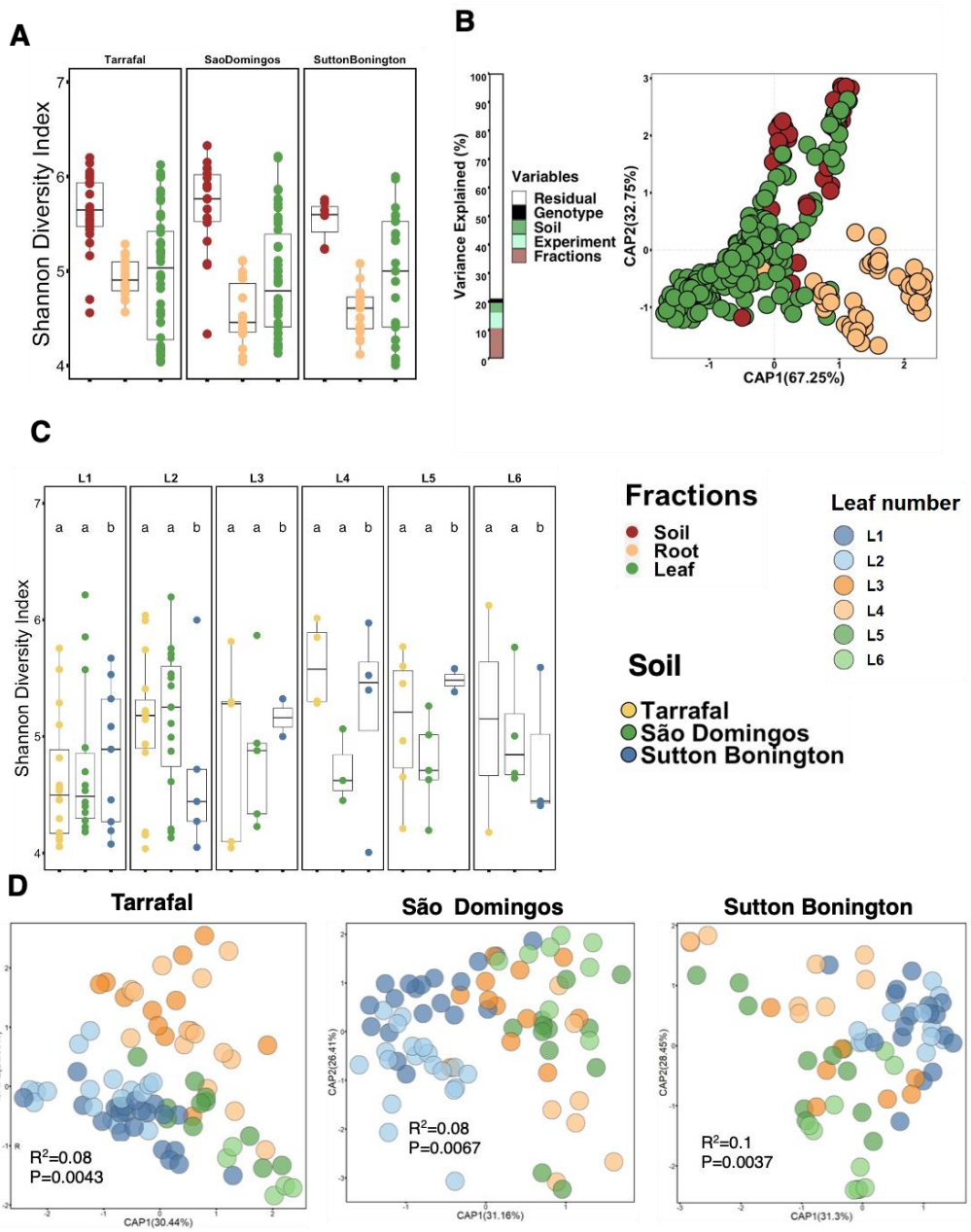

Figure 4: Individual leaf microbiomes. (A) Bacterial alpha diversity estimated using the Shannon Diversity index. **(B)** Canonical analysis of principal coordinates (CAP) based on Bray-Curtis dissimilarities between bacterial communities across soil, root, and shoot. The bar graph to the left of the CAP depicts the percentage of variance explained by statistically significant ($p < 0.05$) variable in a PERMANOVA model. **(C)** Leaf number displayed reproducible effect on bacterial α-diversity. Each panel represents bacterial α-diversity across the different leaves. Bacterial α-diversity was estimated using Shannon diversity index. Letters represents statistical significance corresponding to ANOVA with Tukey's HSD *post hoc* test ($\alpha = 0.05$). **(D)** Canonical analysis of principal coordinates (CAP) based on Bray-Curtis dissimilarities showing the influence of leaf number on the assembly of the bacterial community across plants grown in the 3 different soils described here. Different colours differentiate between the leaves. PERMANOVA R^2 and p-value

(P) are shown within each plot. All samples are biologically independent and represent two independent experiment (Tarrafal, n = 60 leaves. São Domingos, n = 60 leaves. Sutton Bonington, n = 60 leaves).

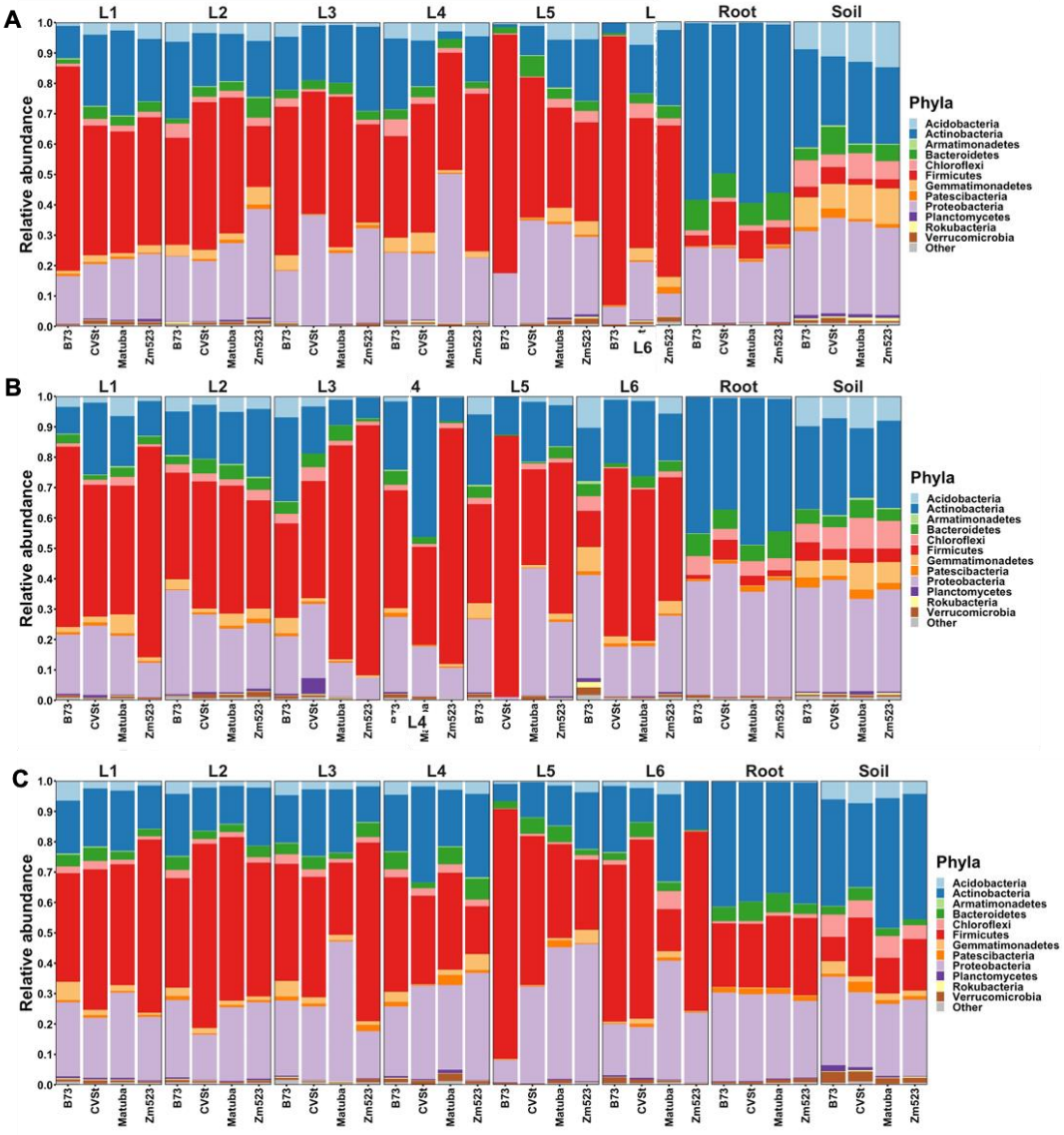

Figure 5: Relative abundance profiles of the main phyla found across the soils. (A) Tarrafal **(B)** São Domingos (C) Sutton Bonington. Plot are coloured by phylum. The numbers in L1 to L6 refer to the positions of leaves according to their order of appearance.

5 Conclusions and future perspectives

Plant growth is complex, dynamic and multifactorial, our study demonstrates that external cues, such as soil mineral content and soil microbiota have a differential effect on root and shoot growth and biomass. Moreover, we found that individual leaves respond differentially to those external cues.

Soil mineral composition has been described as one of the main factors that explains variation in leaf ionome composition (Stein et al., 2017). Our ionome analysis revealed that different leaves represent a distinct ionome profile that is reproducible independently of the soil mineral content. This differential response of leaves to external cues has been described in the context of plant immunity (Berens et al., 2019). Since, bacterial communities play an important role in plant development and growth, we cannot exclude that the leaf ionome findings and the reported differential leaf immunity may differentially affect leaf-associated bacteria. The data show that different leaves harbour different bacterial communities. Factors and mechanisms determining microbiota structure and contributions to plant growth are beginning to be defined (Hou et al., 2020; Salas-González et al., 2020). In the context of the observed differential leaf ionome and microbiome, this raises the intriguing possibility that each leaf within a plant is a distinct habitat having an adapted corresponding distinctive leaf-resident community. This adaptation could be through several mechanisms such as ability to extract nutrients, production of hormones and surfactants, as well as motility and biofilm formation (Nadakuduti et al., 2012; Ueda et al., 2018; Leveau, 2019; Oso et al., 2019).

In conclusion, my work here describes the importance of leaf-environment in selecting different microbial communities in plants, likely modulating plant growth in natural environment. This opens the possibility to develop microbial-based strategies to control plant growth at the organ level, raising opportunities to improve plant edible parts without affecting their nutritional content. Therefore, to reach this final goal, further studies are required to understand the individual mechanisms operating in each leaf and disclosing if these mechanisms are retained in different microbial habitats such as soil, flowers and seeds with similar nutrient composition.

6 References

Achard, P., Gusti, A., Cheminant, S., Alioua, M., Dhondt, S., Coppens, F., et al. (2009). Gibberellin Signaling Controls Cell Proliferation Rate in Arabidopsis. *Current Biology* 19, 1188–1193. doi:10.1016/J.CUB.2009.05.059.

Aichinger, E., Kornet, N., Friedrich, T., and Laux, T. (2012). Plant stem cell niches. *Annu Rev Plant Biol* 63, 615–636. doi:10.1146/ANNUREV-ARPLANT-042811-105555.

Bai, Y., Müller, D. B., Srinivas, G., Garrido-Oter, R., Potthoff, E., Rott, M., et al. (2015). Functional overlap of the Arabidopsis leaf and root microbiota. *Nature* 528, 364–369. doi:10.1038/nature16192.

Bailly, A., Groenhagen, U., Schulz, S., Geisler, M., Eberl, L., and Weisskopf, L. (2014). The inter-kingdom volatile signal indole promotes root development by interfering with auxin signalling. *The Plant Journal* 80, 758–771. doi:10.1111/TPJ.12666.

Baptista, I., Ritsema, C., and Geissen, V. (2015). Effect of Integrated Water-Nutrient Management Strategies on Soil Erosion Mediated Nutrient Loss and Crop Productivity in Cabo Verde Drylands. *PLOS ONE* 10, e0134244. doi:10.1371/journal.pone.0134244.

Bar, M., Ben-Herzel, O., Kohay, H., Shtein, I., and Ori, N. (2015). CLAUSA restricts tomato leaf morphogenesis and GOBLET expression. *The Plant Journal* 83, 888–902. doi:10.1111/TPJ.12936.

Bargmann, B. O. R., Vanneste, S., Krouk, G., Nawy, T., Efroni, I., Shani, E., et al. (2013). A map of cell type-specific auxin responses. *Molecular Systems Biology* 9, 688. doi:10.1038/MSB.2013.40.

Barton, M. K. (2010). Twenty years on: The inner workings of the shoot apical meristem, a developmental dynamo. *Developmental Biology* 341, 95–113. doi:10.1016/J.YDBIO.2009.11.029.

Beemster, G. T. S., De Veylder, L., Vercruysse, S., West, G., Rombaut, D., Van Hummelen, P., et al. (2005). Genome-Wide Analysis of Gene Expression Profiles Associated with Cell Cycle Transitions in Growing Organs of Arabidopsis. *Plant Physiology* 138, 734–743. doi:10.1104/PP.104.053884.

Bellini, C., Pacurar, D. I., and Perrone, I. (2014). Adventitious roots and lateral roots: similarities and differences. *Annu Rev Plant Biol* 65, 639–666. doi:10.1146/ANNUREV-ARPLANT-050213-035645.

Bennett, T., van den Toorn, A., Willemsen, V., and Scheres, B. (2014). Precise control of plant stem cell activity through parallel regulatory inputs. *Development* 141, 4055–4064. doi:10.1242/DEV.110148.

Berendsen, R. L., Pieterse, C. M. J., and Bakker, P. A. H. M. (2012). The rhizosphere microbiome and plant health. *Trends Plant Sci* 17, 478–486. doi:10.1016/J.TPLANTS.2012.04.001.

Berens, M. L., Wolinska, K. W., Spaepen, S., Ziegler, J., Nobori, T., Nair, A., et al. (2019). Balancing trade-offs between biotic and abiotic stress responses through leaf age-dependent variation in stress hormone cross-talk. *Proc Natl Acad Sci U S A* 116, 2364–2373. doi:10.1073/pnas.1817233116.

Berg, G. Plant-microbe interactions promoting plant growth and health: perspectives for controlled use of microorganisms in agriculture. doi:10.1007/s00253-009-2092-7.

Bowman, J. L., Eshed, Y., and Baum, S. F. (2002). Establishment of polarity in angiosperm lateral organs. *Trends in Genetics* 18, 134–141. doi:10.1016/S0168-9525(01)02601-4.

Bowman, J. L., and Floyd, S. K. (2008). Patterning and Polarity in Seed Plant Shoots. *http://dx.doi.org/10.1146/annurev.arplant.57.032905.105356* 59, 67–88. doi:10.1146/ANNUREV.ARPLANT.57.032905.105356.

Breeze, E., Harrison, E., McHattie, S., Hughes, L., Hickman, R., Hill, C., et al. (2011). High-Resolution Temporal Profiling of Transcripts during Arabidopsis Leaf Senescence Reveals a Distinct Chronology of Processes and Regulation. *The Plant Cell* 23, 873–894. doi:10.1105/TPC.111.083345.

Caggiano, M. P., Yu, X., Bhatia, N., Larsson, A., Ram, H., Ohno, C. K., et al. (2017). Cell type boundaries organize plant development. *Elife* 6. doi:10.7554/eLife.27421.

Callahan, B. J., McMurdie, P. J., Rosen, M. J., Han, A. W., Johnson, A. J. A., and Holmes, S. P. (2016). DADA2: High-resolution sample inference from Illumina amplicon data. *Nature Methods*. doi:10.1038/nmeth.3869.

Castrillo, G., Teixeira, P. J. P. L., Paredes, S. H., Law, T. F., de Lorenzo, L., Feltcher, M. E., et al. (2017). Root microbiota drive direct integration of phosphate stress and immunity. *Nature* 543, 513–518. doi:10.1038/nature21417.

Chaiwanon, J., and Wang, Z. Y. (2015). Spatiotemporal Brassinosteroid Signaling and Antagonism with Auxin Pattern Stem Cell Dynamics in Arabidopsis Roots. *Current Biology* 25, 1031–1042. doi:10.1016/J.CUB.2015.02.046.

Chen, J., Xu, W., Velten, J., Xin, Z., and Stout, J. (2012). Characterization of maize inbred lines for drought and heat tolerance. *Journal of Soil and Water Conservation* 67, 354–364. doi:10.2489/jswc.67.5.354.

Chen, J., Zhao, G., Wei, Y., Dong, Y., Hou, L., and Jiao, R. (2021). Isolation and screening of multifunctional phosphate solubilizing bacteria and its growth-promoting effect on Chinese fir seedlings. *Scientific Reports 2021 11:1* 11, 1–13. doi:10.1038/s41598-021-88635-4.

Chiu, C. H., and Paszkowski, U. (2019). Mechanisms and Impact of Symbiotic Phosphate Acquisition. *Cold Spring Harbor Perspectives in Biology* 11, a034603. doi:10.1101/CSHPERSPECT.A034603.

Choe, S., Fujioka, S., Noguchi, T., Takatsuto, S., Yoshida, S., and Feldmann, K. A. (2001a). Overexpression of DWARF4 in the brassinosteroid biosynthetic pathway results in increased vegetative growth and seed yield in Arabidopsis. *Plant Journal* 26, 573–582. doi:10.1046/J.1365-313X.2001.01055.X.

Choe, S., Fujioka, S., Noguchi, T., Takatsuto, S., Yoshida, S., and Feldmann, K. A. (2001b). Overexpression of DWARF4 in the brassinosteroid biosynthetic pathway results in increased vegetative growth and seed yield in Arabidopsis. *The Plant Journal* 26, 573–582. doi:10.1046/J.1365-313X.2001.01055.X.

Chung, Y., Zhu, Y., Wu, M. F., Simonini, S., Kuhn, A., Armenta-Medina, A., et al. (2019). Auxin Response Factors promote organogenesis by chromatin-mediated repression of the pluripotency gene SHOOTMERISTEMLESS. *Nature Communications 2019 10:1* 10, 1–11. doi:10.1038/s41467-019-08861-3.

Clauw, P., Coppens, F., de Beuf, K., Dhondt, S., van Daele, T., Maleux, K., et al. (2015). Leaf responses to mild drought stress in natural variants of Arabidopsis. *Plant Physiol* 167, 800–816. doi:10.1104/PP.114.254284.

Cubas, P., Lauter, N., Doebley, J., and Coen, E. (1999). The TCP domain: a motif found in proteins regulating plant growth and development. *The Plant Journal* 18, 215–222. doi:10.1046/J.1365-313X.1999.00444.X.

Danish, S., Zafar-Ul-Hye, M., Mohsin, F., and Hussain, M. (2020). ACC-deaminase producing plant growth promoting rhizobacteria and biochar mitigate adverse effects of drought stress on maize growth. *PLOS ONE* 15, e0230615. doi:10.1371/JOURNAL.PONE.0230615.

De Wit, M., Galvão, V. C., and Fankhauser, C. (2016). Light-Mediated Hormonal Regulation of Plant Growth and Development. doi:10.1146/annurev-arplant-043015-112252.

Debernardi, J. M., Mecchia, M. A., Vercruyssen, L., Smaczniak, C., Kaufmann, K., Inze, D., et al. (2014). Post-transcriptional control of GRF transcription factors by microRNA miR396 and GIF co-activator affects leaf size and longevity. *The Plant Journal* 79, 413–426. doi:10.1111/TPJ.12567.

Delgado-Baquerizo, M., Oliverio, A. M., Brewer, T. E., Benavent-González, A., Eldridge, D. J., Bardgett, R. D., et al. (2018). A global atlas of the dominant bacteria found in soil. *Science (1979)* 359, 320–325. doi:10.1126/science.aap9516.

Delgado-Baquerizo, M., Reich, P. B., Trivedi, C., Eldridge, D. J., Abades, S., Alfaro, F. D., et al. (2020). Multiple elements of soil biodiversity drive ecosystem functions across biomes. *Nature Ecology and Evolution* 4, 210–220. doi:10.1038/s41559-019-1084-y.

Dengler, N. G., and Tsukaya, H. (2001). Leaf Morphogenesis in Dicotyledons: Current Issues. *https://doi.org/10.1086/320145* 162, 459–464. doi:10.1086/320145.

Di Mambro, R., De Ruvo, M., Pacifici, E., Salvi, E., Sozzani, R., Benfey, P. N., et al. (2017). Auxin minimum triggers the developmental switch from cell division to cell differentiation in the Arabidopsis root. *Proc Natl Acad Sci U S A* 114, E7641–E7649. doi:10.1073/PNAS.1705833114/SUPPL_FILE/PNAS.1705833114.SAPP.PDF.

Dolan, L., Janmaat, K., Willemsen, V., Linstead, P., Poethig, S., Roberts, K., et al. (1993). Cellular organisation of the Arabidopsis thaliana root. *Development* 119, 71–84. doi:10.1242/DEV.119.1.71.

Donnelly, P. M., Bonetta, D., Tsukaya, H., Dengler, R. E., and Dengler, N. G. (1999). Cell Cycling and Cell Enlargement in Developing Leaves of Arabidopsis. *Developmental Biology* 215, 407–419. doi:10.1006/DBIO.1999.9443.

Du, F., Guan, C., and Jiao, Y. (2018). Molecular Mechanisms of Leaf Morphogenesis. *Molecular Plant* 11, 1117–1134. doi:10.1016/J.MOLP.2018.06.006.

Dubois, M., Claeys, H., van den Broeck, L., and Inzé, D. (2017). Time of day determines Arabidopsis transcriptome and growth dynamics under mild drought. *Plant, Cell & Environment* 40, 180–189. doi:10.1111/PCE.12809.

Durán, P., Thiergart, T., Garrido-Oter, R., Agler, M., Kemen, E., Schulze-Lefert, P., et al. (2018). Microbial Interkingdom Interactions in Roots Promote Arabidopsis Survival. *Cell* 175, 973-983.e14. doi:10.1016/j.cell.2018.10.020.

Emery, J. F., Floyd, S. K., Alvarez, J., Eshed, Y., Hawker, N. P., Izhaki, A., et al. (2003). Radial Patterning of Arabidopsis Shoots by Class III HD-ZIP and KANADI Genes. *Current Biology* 13, 1768–1774. doi:10.1016/J.CUB.2003.09.035.

Eshed, Y., Baum, S. F., Perea, J. V., and Bowman, J. L. (2001). Establishment of polarity in lateral organs of plants. *Current Biology* 11, 1251–1260. doi:10.1016/S0960-9822(01)00392-X.

Fierer, N., Lauber, C. L., Ramirez, K. S., Zaneveld, J., Bradford, M. A., and Knight, R. (2012). Comparative metagenomic, phylogenetic and physiological analyses of soil microbial communities across nitrogen gradients. *ISME Journal*. doi:10.1038/ismej.2011.159.

Finkel, O. M., Salas-González, I., Castrillo, G., Conway, J. M., Law, T. F., Teixeira, P. J. P. L., et al. (2020). A single bacterial genus maintains root growth in a complex microbiome. *Nature 2020 587:7832* 587, 103–108. doi:10.1038/s41586-020-2778-7.

Finkel, O. M., Salas-González, I., Castrillo, G., Spaepen, S., Law, T. F., Teixeira, P. J. P. L., et al. (2019). The effects of soil phosphorus content on plant microbiota are driven by the plant phosphate starvation response. *PLoS Biology*. doi:10.1371/journal.pbio.3000534.

Forzani, C., Aichinger, E., Sornay, E., Willemsen, V., Laux, T., Dewitte, W., et al. (2014). WOX5 Suppresses CYCLIN D Activity to Establish Quiescence at the Center of the Root Stem Cell Niche. *Current Biology* 24, 1939–1944. doi:10.1016/J.CUB.2014.07.019.

Fournier, C., Durand, J. L., Ljutovac, S., Schäufele, R., Gastal, F., and Andrieu, B. (2005). A functional–structural model of elongation of the grass leaf and its relationships with the phyllochron. *New Phytologist* 166, 881–894. doi:10.1111/J.1469-8137.2005.01371.X.

Gonzalez, N., de Bodt, S., Sulpice, R., Jikumaru, Y., Chae, E., Dhondt, S., et al. (2010). Increased Leaf Size: Different Means to an End. *Plant Physiology* 153, 1261–1279. doi:10.1104/PP.110.156018.

Goteti, P. K., Emmanuel, L. D. A., Desai, S., and Shaik, M. H. A. (2013). Prospective zinc solubilising bacteria for enhanced nutrient uptake and growth promotion in maize (Zea mays L.). *International Journal of Microbiology* 2013. doi:10.1155/2013/869697.

Gouda, S., Kerry, R. G., Das, G., Paramithiotis, S., Shin, H. S., and Patra, J. K. (2018). Revitalization of plant growth promoting rhizobacteria for sustainable development in agriculture. *Microbiological Research* 206, 131–140. doi:10.1016/J.MICRES.2017.08.016.

Grieneisen, V. A., Xu, J., Marée, A. F. M., Hogeweg, P., and Scheres, B. (2007). Auxin transport is sufficient to generate a maximum and gradient guiding root growth. *Nature* 449, 1008–1013. doi:10.1038/NATURE06215.

Gu, S., Wei, Z., Shao, Z., Friman, V. P., Cao, K., Yang, T., et al. (2020). Competition for iron drives phytopathogen control by natural rhizosphere microbiomes. *Nature Microbiology* 5, 1002–1010. doi:10.1038/s41564-020-0719-8.

Guo, H., Li, L., Aluru, M., Aluru, S., and Yin, Y. (2013). Mechanisms and networks for brassinosteroid regulated gene expression. *Current Opinion in Plant Biology* 16, 545–553. doi:10.1016/J.PBI.2013.08.002.

Ha, C. M., Ji, H. J., Hong, G. N., and Fletcher, J. C. (2007). BLADE-ON-PETIOLE1 and 2 control Arabidopsis lateral organ fate through regulation of LOB domain and adaxial-abaxial polarity genes. *Plant Cell* 19, 1809–1825. doi:10.1105/tpc.107.051938.

Ha, C. M., Jun, J. H., and Fletcher, J. C. (2010). Control of Arabidopsis Leaf Morphogenesis Through Regulation of the YABBY and KNOX Families of Transcription Factors. *Genetics* 186, 197–206. doi:10.1534/GENETICS.110.118703.

Hacquard, S., Spaepen, S., Garrido-Oter, R., and Schulze-Lefert, P. (2017). Interplay Between Innate Immunity and the Plant Microbiota. *Annu Rev Phytopathol* 55, 565–589. doi:10.1146/ANNUREV-PHYTO-080516-035623.

Harbort, C. J., Hashimoto, M., Inoue, H., Niu, Y., Guan, R., Rombolà, A. D., et al. (2020a). Root-Secreted Coumarins and the Microbiota Interact to Improve Iron Nutrition in Arabidopsis. *Cell Host Microbe* 28, 825-837.e6. doi:10.1016/j.chom.2020.09.006.

Harbort, C. J., Hashimoto, M., Inoue, H., Niu, Y., Guan, R., Rombolà, A. D., et al. (2020b). Root-Secreted Coumarins and the Microbiota Interact to Improve

Iron Nutrition in Arabidopsis. *Cell Host & Microbe* 28, 825-837.e6. doi:10.1016/J.CHOM.2020.09.006.

He, M., Yan, Z., Cui, X., Gong, Y., Li, K., and Han, W. (2020). Scaling the leaf nutrient resorption efficiency: Nitrogen vs phosphorus in global plants. *Science of The Total Environment* 729, 138920. doi:10.1016/J.SCITOTENV.2020.138920.

Heidstra, R., and Sabatini, S. (2014). Plant and animal stem cells: similar yet different. *Nature Reviews Molecular Cell Biology 2014 15:5* 15, 301–312. doi:10.1038/nrm3790.

Heisler, M. G., Ohno, C., Das, P., Sieber, P., Reddy, G. v., Long, J. A., et al. (2005). Patterns of auxin transport and gene expression during primordium development revealed by live imaging of the Arabidopsis inflorescence meristem. *Curr Biol* 15, 1899–1911. doi:10.1016/J.CUB.2005.09.052.

Helfrich, E. J. N., Vogel, C. M., Ueoka, R., Schäfer, M., Ryffel, F., Müller, D. B., et al. (2018). Bipartite interactions, antibiotic production and biosynthetic potential of the Arabidopsis leaf microbiome. *Nature Microbiology 2018 3:8* 3, 909–919. doi:10.1038/s41564-018-0200-0.

Hilo, A., Shahinnia, F., Druege, U., Franken, P., Melzer, M., Rutten, T., et al. (2017). A specific role of iron in promoting meristematic cell division during adventitious root formation. *Journal of Experimental Botany* 68, 4233–4247. doi:10.1093/jxb/erx248.

Hiruma, K., Gerlach, N., Sacristán, S., Nakano, R. T., Hacquard, S., Kracher, B., et al. (2016). Root Endophyte Colletotrichum tofieldiae Confers Plant Fitness Benefits that Are Phosphate Status Dependent. *Cell* 165, 464–74. doi:10.1016/j.cell.2016.02.028.

Hou, S., Thiergart, T., Vannier, N., Mesny, F., Ziegler, J., Pickel, B., et al. (2020). Microbiota-root-shoot axis modulation by MYC2 favours arabidopsis growth over defence under suboptimal light. *bioRxiv*, 1–29. doi:10.1101/2020.11.06.371146.

Huang, S., Raman, A. S., Ream, J. E., Fujiwara, H., Eric Cerny, R., and Brown, S. M. (1998). Overexpression of 20-Oxidase Confers a Gibberellin-

Overproduction Phenotype in Arabidopsis. *Plant Physiology* 118, 773–781. doi:10.1104/PP.118.3.773.

Huang, T., Harrar, Y., Lin, C., Reinhart, B., Newell, N. R., Talavera-Rauh, F., et al. (2014). Arabidopsis KANADI1 Acts as a Transcriptional Repressor by Interacting with a Specific cis-Element and Regulates Auxin Biosynthesis, Transport, and Signaling in Opposition to HD-ZIPIII Factors. *The Plant Cell* 26, 246–262. doi:10.1105/TPC.113.111526.

Ishida, H., Izumi, M., Wada, S., and Makino, A. (2014). Roles of autophagy in chloroplast recycling. *Biochimica et Biophysica Acta (BBA) - Bioenergetics* 1837, 512–521. doi:10.1016/J.BBABIO.2013.11.009.

Jain, D., Kour, R., Bhojiya, A. A., Meena, R. H., Singh, A., Mohanty, S. R., et al. (2020). Zinc tolerant plant growth promoting bacteria alleviates phytotoxic effects of zinc on maize through zinc immobilization. *Scientific Reports 2020 10:1* 10, 1–13. doi:10.1038/s41598-020-70846-w.

Jasinski, S., Piazza, P., Craft, J., Hay, A., Woolley, L., Rieu, I., et al. (2005). KNOX action in Arabidopsis is mediated by coordinate regulation of cytokinin and gibberellin activities. *Curr Biol* 15, 1560–1565. doi:10.1016/J.CUB.2005.07.023.

Johnston, R., Leiboff, S., and Scanlon, M. J. (2015). Ontogeny of the sheathing leaf base in maize (Zea mays). *New Phytologist* 205, 306–315. doi:10.1111/NPH.13010/FORMAT/PDF.

Kalve, S., De Vos, D., and Beemster, G. T. S. (2014). Leaf development: A cellular perspective. *Frontiers in Plant Science* 5, 362. doi:10.3389/FPLS.2014.00362/BIBTEX.

Kerstetter, R. A., Bollman, K., Taylor, R. A., Bomblies, K., and Poethig, R. S. (2001). KANADI regulates organ polarity in Arabidopsis. *Nature 2001 411:6838* 411, 706–709. doi:10.1038/35079629.

Kidner, C. A., and Timmermans, M. C. (2007). Mixing and matching pathways in leaf polarity. *Curr Opin Plant Biol* 10, 13–20. doi:10.1016/J.PBI.2006.11.013.

Koch, M., Winkelmann, M. K., Hasler, M., Pawelzik, E., and Naumann, M. (2020). Root growth in light of changing magnesium distribution and transport

between source and sink tissues in potato (Solanum tuberosum L.). *Scientific Reports 2020 10:1* 10, 1–14. doi:10.1038/s41598-020-65896-z.

Lauber, C. L., Hamady, M., Knight, R., and Fierer, N. (2009). Pyrosequencing-Based Assessment of Soil pH as a Predictor of Soil Bacterial Community Structure at the Continental Scale †. *APPLIED AND ENVIRONMENTAL MICROBIOLOGY* 75, 5111–5120. doi:10.1128/AEM.00335-09.

Lebeis, S. L., Paredes, S. H., Lundberg, D. S., Glavina, T., and Jones, C. D. (2015). Salicylic acid modulates colonization of the root microbiome by specific bacterial taxa. 349, 1678–1681. doi:10.5061/dryad.238b2.

Lee, B. H., Ko, J. H., Lee, S., Lee, Y., Pak, J. H., and Kim, J. H. (2009). The Arabidopsis GRF-INTERACTING FACTOR gene family performs an overlapping function in determining organ size as well as multiple developmental properties. *Plant Physiol* 151, 655–668. doi:10.1104/PP.109.141838.

Leff, J. W., Jones, S. E., Prober, S. M., Barberán, A., Borer, E. T., Firn, J. L., et al. (2015). Consistent responses of soil microbial communities to elevated nutrient inputs in grasslands across the globe. *Proc Natl Acad Sci U S A* 112, 10967–10972. doi:10.1073/pnas.1508382112.

Leveau, J. H. (2019). A brief from the leaf: latest research to inform our understanding of the phyllosphere microbiome. *Current Opinion in Microbiology* 49, 41–49. doi:10.1016/j.mib.2019.10.002.

Li, Z., Li, B., Shen, W. H., Huang, H., and Dong, A. (2012). TCP transcription factors interact with AS2 in the repression of class-I KNOX genes in Arabidopsis thaliana. *The Plant Journal* 71, 99–107. doi:10.1111/J.1365-313X.2012.04973.X.

Li, Z., Zhang, Y., Zou, D., Zhao, Y., Wang, H. L., Zhang, Y., et al. (2020). LSD 3.0: a comprehensive resource for the leaf senescence research community. *Nucleic Acids Research* 48, D1069–D1075. doi:10.1093/NAR/GKZ898.

Liu, D., Song, Y., Chen, Z., and Yu, D. (2009). Ectopic expression of miR396 suppresses GRF target gene expression and alters leaf growth in

Arabidopsis. *Physiologia Plantarum* 136, 223–236. doi:10.1111/J.1399-3054.2009.01229.X.

Liu, J., Sheng, L., Xu, Y., Li, J., Yang, Z., Huang, H., et al. (2014). WOX11 and 12 Are Involved in the First-Step Cell Fate Transition during de Novo Root Organogenesis in Arabidopsis. *The Plant Cell* 26, 1081–1093. doi:10.1105/TPC.114.122887.

Lornac, A., Havé, M., Chardon, F., Soulay, F., Clément, G., Avice, J. C., et al. (2020). Autophagy Controls Sulphur Metabolism in the Rosette Leaves of Arabidopsis and Facilitates S Remobilization to the Seeds. *Cells* 9. doi:10.3390/CELLS9020332.

Love, M. I., Huber, W., and Anders, S. (2014). Moderated estimation of fold change and dispersion for RNA-seq data with DESeq2. *Genome Biology* 15, 550. doi:10.1186/s13059-014-0550-8.

Martin, M. (2011). Cutadapt removes adapter sequences from high-throughput sequencing reads. *EMBnet J*. doi:10.14806/ej.17.1.200.

Martins, S., Montiel-Jorda, A., Cayrel, A., Huguet, S., Roux, C. P.-L., Ljung, K., et al. (2017). Brassinosteroid signaling-dependent root responses to prolonged elevated ambient temperature. *Nature Communications 2017 8:1* 8, 1–11. doi:10.1038/s41467-017-00355-4.

McConnell, J. R., Emery, J., Eshed, Y., Bao, N., Bowman, J., and Barton, M. K. (2001). Role of PHABULOSA and PHAVOLUTA in determining radial patterning in shoots. *Nature* 411, 709–713. doi:10.1038/35079635.

Mendes, R., Garbeva, P., and Raaijmakers, J. M. (2013). The rhizosphere microbiome: significance of plant beneficial, plant pathogenic, and human pathogenic microorganisms. *FEMS Microbiology Reviews* 37, 634–663. doi:10.1111/1574-6976.12028.

Motte, H., Vanneste, S., and Beeckman, T. (2019). Molecular and Environmental Regulation of Root Development. *Annu Rev Plant Biol* 70, 465–488. doi:10.1146/ANNUREV-ARPLANT-050718-100423.

Moubayidin, L., Perilli, S., dello Ioio, R., di Mambro, R., Costantino, P., and Sabatini, S. (2010). The Rate of Cell Differentiation Controls the Arabidopsis

Root Meristem Growth Phase. *Current Biology* 20, 1138–1143. doi:10.1016/J.CUB.2010.05.035.

Nadakuduti, S. S., Pollard, M., Kosma, D. K., Allen, C., Ohlrogge, J. B., and Barry, C. S. (2012). Pleiotropic phenotypes of the sticky peel mutant provide new insight into the role of CUTIN DEFICIENT2 in epidermal cell function in tomato. *Plant Physiology* 159, 945–960. doi:10.1104/pp.112.198374.

Oksanen, J. (2007). vegan : Community Ecology Package. R package version 1.8-5.

Omary, M., Gil-Yarom, N., Yahav, C., Steiner, E., Hendelman, A., and Efroni, I. (2022). A conserved superlocus regulates above- and belowground root initiation. *Science (1979)* 375. doi:10.1126/SCIENCE.ABF4368.

Ori, N., Cohen, A. R., Etzioni, A., Brand, A., Yanai, O., Shleizer, S., et al. (2007). Regulation of LANCEOLATE by miR319 is required for compound-leaf development in tomato. *Nature Genetics 2007 39:6* 39, 787–791. doi:10.1038/ng2036.

Oso, S., Walters, M., Schlechter, R. O., and Remus-Emsermann, M. N. P. (2019). Utilisation of hydrocarbons and production of surfactants by bacteria isolated from plant leaf surfaces. *FEMS Microbiology Letters* 366, 61. doi:10.1093/femsle/fnz061.

Otegui, M. S. (2018). Vacuolar degradation of chloroplast components: autophagy and beyond. *Journal of Experimental Botany* 69, 741–750. doi:10.1093/JXB/ERX234.

Palatnik, J. F., Allen, E., Wu, X., Schommer, C., Schwab, R., Carrington, J. C., et al. (2003). Control of leaf morphogenesis by microRNAs. *Nature 2003 425:6955* 425, 257–263. doi:10.1038/nature01958.

Pandey, S., and Gupta, S. (2020). Evaluation of Pseudomonas sp. for its multifarious plant growth promoting potential and its ability to alleviate biotic and abiotic stress in tomato (Solanum lycopersicum) plants. *Scientific Reports 2020 10:1* 10, 1–15. doi:10.1038/s41598-020-77850-0.

Pantin, F., Simonneau, T., and Muller, B. (2012). Coming of leaf age: control of growth by hydraulics and metabolics during leaf ontogeny. *New Phytologist* 196, 349–366. doi:10.1111/J.1469-8137.2012.04273.X.

Parent, B., Turc, O., Gibon, Y., Stitt, M., and Tardieu, F. (2010). Modelling temperature-compensated physiological rates, based on the co-ordination of responses to temperature of developmental processes. *Journal of Experimental Botany* 61, 2057–2069. doi:10.1093/JXB/ERQ003.

Peng, X., Yang, Y., Yan, X., and Li, H. (2021). The effects of water control on the survival and growth of Alternanthera philoxeroides in the vegetative reproduction and seedling stages. *Scientific Reports 2021 11:1* 11, 1–10. doi:10.1038/s41598-021-92674-2.

Petrášek, J., and Friml, J. (2009). Auxin transport routes in plant development. *Development* 136, 2675–2688. doi:10.1242/DEV.030353.

Pieterse, C. M. J., Zamioudis, C., Berendsen, R. L., Weller, D. M., van Wees, S. C. M., Bakker, P. A. H. M., et al. (2014). Induced Systemic Resistance by Beneficial Microbes. *http://dx.doi.org/10.1146/annurev-phyto-082712-102340* 52, 347–375. doi:10.1146/ANNUREV-PHYTO-082712-102340.

Poethig, R. S. (2013). Vegetative phase change and shoot maturation in plants. *Curr Top Dev Biol* 105, 125–152. doi:10.1016/B978-0-12-396968-2.00005-1.

Qi, J., Wu, B., Feng, S., Lü, S., Guan, C., Zhang, X., et al. (2017). Mechanical regulation of organ asymmetry in leaves. *Nature Plants 2017 3:9* 3, 724–733. doi:10.1038/s41477-017-0008-6.

Quast, C., Pruesse, E., Yilmaz, P., Gerken, J., Schweer, T., Yarza, P., et al. (2013). The SILVA ribosomal RNA gene database project: Improved data processing and web-based tools. *Nucleic Acids Research* 41. doi:10.1093/nar/gks1219.

Raaijmakers, J. M., and Mazzola, M. (2012). Diversity and natural functions of antibiotics produced by beneficial and plant pathogenic bacteria. *Annu Rev Phytopathol* 50, 403–424. doi:10.1146/ANNUREV-PHYTO-081211-172908.

Rao, L., Li, S., and Cui, X. (2021). Leaf morphology and chlorophyll fluorescence characteristics of mulberry seedlings under waterlogging stress. *Scientific Reports 2021 11:1* 11, 1–11. doi:10.1038/s41598-021-92782-z.

Reinhardt, D., Pesce, E. R., Stieger, P., Mandel, T., Baltensperger, K., Bennett, M., et al. (2003). Regulation of phyllotaxis by polar auxin transport. *Nature 2003 426:6964* 426, 255–260. doi:10.1038/nature02081.

Reinhart, B. J., Liu, T., Newell, N. R., Magnani, E., Huang, T., Kerstetter, R., et al. (2013). Establishing a Framework for the Ad/Abaxial Regulatory Network of Arabidopsis: Ascertaining Targets of Class III HOMEODOMAIN LEUCINE ZIPPER and KANADI Regulation. *The Plant Cell* 25, 3228–3249. doi:10.1105/TPC.113.111518.

Richardson, A. E., and Simpson, R. J. (2011). Soil Microorganisms Mediating Phosphorus Availability Update on Microbial Phosphorus. *Plant Physiology* 156, 989–996. doi:10.1104/PP.111.175448.

Ritpitakphong, U., Falquet, L., Vimoltust, A., Berger, A., Métraux, J. P., and L'Haridon, F. (2016). The microbiome of the leaf surface of Arabidopsis protects against a fungal pathogen. *New Phytologist* 210, 1033–1043. doi:10.1111/NPH.13808.

Rodriguez, R. E., Mecchia, M. A., Debernardi, J. M., Schommer, C., Weigel, D., and Palatnik, J. F. (2010). Control of cell proliferation in Arabidopsis thaliana by microRNA miR396. *Development* 137, 103–112. doi:10.1242/DEV.043067/-/DC1.

Rolli, E., Marasco, R., Vigani, G., Ettoumi, B., Mapelli, F., Deangelis, M. L., et al. (2015). Improved plant resistance to drought is promoted by the root-associated microbiome as a water stress-dependent trait. *Environmental Microbiology* 17, 316–331. doi:10.1111/1462-2920.12439/SUPPINFO.

Sablowski, R. (2011). Plant stem cell niches: from signalling to execution. *Curr Opin Plant Biol* 14, 4–9. doi:10.1016/J.PBI.2010.08.001.

Salas-González, I., Reyt, G., Flis, P., Custódio, V., Gopaulchan, D., Bakhoum, N., et al. (2020). Coordination between microbiota and root endodermis

supports plant mineral nutrient homeostasis. *Science (1979)*, eabd0695. doi:10.1126/science.abd0695.

Salas-González, I., Reyt, G., Flis, P., Custódio, V., Gopaulchan, D., Bakhoum, N., et al. (2021). Coordination between microbiota and root endodermis supports plant mineral nutrient homeostasis. *Science (1979)* 371. doi:10.1126/science.abd0695.

Salt, D. E., Baxter, I., and Lahner, B. (2008). Ionomics and the study of the plant ionome. *Annual Review of Plant Biology* 59, 709–733. doi:10.1146/annurev.arplant.59.032607.092942.

Salvi, E., Rutten, J. P., di Mambro, R., Polverari, L., Licursi, V., Negri, R., et al. (2020). A Self-Organized PLT/Auxin/ARR-B Network Controls the Dynamics of Root Zonation Development in Arabidopsis thaliana. *Developmental Cell* 53, 431-443.e23. doi:10.1016/J.DEVCEL.2020.04.004.

Santos-Medellín, C., Edwards, J., Liechty, Z., Nguyen, B., and Sundaresan, V. (2017). Drought stress results in a compartment-specific restructuring of the rice root-associated microbiomes. *mBio* 8, 764–781. doi:10.1128/mBio.00764-17.

Sarkar, A. K., Luijten, M., Miyashima, S., Lenhard, M., Hashimoto, T., Nakajima, K., et al. (2007). Conserved factors regulate signalling in Arabidopsis thaliana shoot and root stem cell organizers. *Nature 2007 446:7137* 446, 811–814. doi:10.1038/nature05703.

Sarojam, R., Sappl, P. G., Goldshmidt, A., Efroni, I., Floyd, S. K., Eshed, Y., et al. (2010). Differentiating Arabidopsis Shoots from Leaves by Combined YABBY Activities. *The Plant Cell* 22, 2113–2130. doi:10.1105/TPC.110.075853.

Scheres, B., Benfey, P., and Dolan, L. (2002). Root Development. *The Arabidopsis Book / American Society of Plant Biologists* 1, e0101. doi:10.1199/TAB.0101.

Schneider, C. A., Rasband, W. S., and Eliceiri, K. W. (2012). NIH Image to ImageJ: 25 years of image analysis. *Nature Methods* 9, 671–675. doi:10.1038/nmeth.2089.

Schwember, A. R., Schulze, J., del Pozo, A., and Cabeza, R. A. (2019). Regulation of Symbiotic Nitrogen Fixation in Legume Root Nodules. *Plants 2019, Vol. 8, Page 333* 8, 333. doi:10.3390/PLANTS8090333.

Sharma, A., Johri, B. N., Sharma, A. K., and Glick, B. R. (2003). Plant growth-promoting bacterium Pseudomonas sp. strain GRP3 influences iron acquisition in mung bean (Vigna radiata L. Wilzeck). *Soil Biology and Biochemistry* 35, 887–894. doi:10.1016/S0038-0717(03)00119-6.

Shi, C.-L., Park, H.-B., Lee, J. S., Ryu, S., and Ryu, C.-M. (2010). Inhibition of Primary Roots and Stimulation of Lateral Root Development in Arabidopsis thaliana by the Rhizobacterium Serratia marcescens 90-166 Is through Both Auxin-Dependent and-Independent Signaling Pathways. *Mol. Cells* 29, 251–258. doi:10.1007/s10059-010-0032-0.

Smith, S. E., and Smith, F. A. (2011). Roles of Arbuscular Mycorrhizas in Plant Nutrition and Growth: New Paradigms from Cellular to Ecosystem Scales. *http://dx.doi.org/10.1146/annurev-arplant-042110-103846* 62, 227–250. doi:10.1146/ANNUREV-ARPLANT-042110-103846.

Soltanpour, P. N., and Schwab, A. P. (1977). A new soil test for simultaneous extraction of macroand micro-nutrients in alkaline soils. *Communications in Soil Science and Plant Analysis*. doi:10.1080/00103627709366714.

Spaepen, S., Bossuyt, S., Engelen, K., Marchal, K., and Vanderleyden, J. (2014a). Phenotypical and molecular responses of Arabidopsis thaliana roots as a result of inoculation with the auxin-producing bacterium Azospirillum brasilense. *New Phytologist* 201, 850–861. doi:10.1111/NPH.12590.

Spaepen, S., Bossuyt, S., Engelen, K., Marchal, K., and Vanderleyden, J. (2014b). Phenotypical and molecular responses of Arabidopsis thaliana roots as a result of inoculation with the auxin-producing bacterium Azospirillum brasilense. *New Phytol* 201, 850–861. doi:10.1111/NPH.12590.

Spaepen, S., Vanderleyden, J., and Remans, R. (2007). Indole-3-acetic acid in microbial and microorganism-plant signaling. *FEMS Microbiology Reviews* 31, 425–448. doi:10.1111/J.1574-6976.2007.00072.X.

Stahl, Y., and Simon, R. (2010). Plant primary meristems: shared functions and regulatory mechanisms. *Curr Opin Plant Biol* 13, 53–58. doi:10.1016/J.PBI.2009.09.008.

Stahle, M. I., Kuehlich, J., Staron, L., Von Arnim, A. G., and Golz, J. F. (2009). YABBYs and the Transcriptional Corepressors LEUNIG and LEUNIG_HOMOLOG Maintain Leaf Polarity and Meristem Activity in Arabidopsis. *The Plant Cell* 21, 3105. doi:10.1105/TPC.109.070458.

Stein, R. J., Höreth, S., de Melo, J. R. F., Syllwasschy, L., Lee, G., Garbin, M. L., et al. (2017). Relationships between soil and leaf mineral composition are element-specific, environment-dependent and geographically structured in the emerging model Arabidopsis halleri. *New Phytologist* 213, 1274–1286. doi:10.1111/nph.14219.

Taiz, L., Zeiger, E., Møller, I. M., and Murphy, A. (2015). Plant physiology and development. *Plant physiology and development.*

Thierfelder, C., Rusinamhodzi, L., Setimela, P., Walker, F., and Eash, N. S. (2016). Conservation agriculture and drought-tolerant germplasm: Reaping the benefits of climate-smart agriculture technologies in central Mozambique. *Renewable Agriculture and Food Systems* 31, 414–428. doi:10.1017/S1742170515000332.

Tong, H., Xiao, Y., Liu, D., Gao, S., Liu, L., Yin, Y., et al. (2014). Brassinosteroid Regulates Cell Elongation by Modulating Gibberellin Metabolism in Rice. *The Plant Cell* 26, 4376. doi:10.1105/TPC.114.132092.

Truyens, S., Weyens, N., Cuypers, A., and Vangronsveld, J. (2015). Bacterial seed endophytes: genera, vertical transmission and interaction with plants. *Environmental Microbiology Reports* 7, 40–50. doi:10.1111/1758-2229.12181.

Tsuda, K., and Hake, S. (2016). Homeobox Transcription Factors and the Regulation of Meristem Development and Maintenance. *Plant Transcription Factors: Evolutionary, Structural and Functional Aspects*, 215–228. doi:10.1016/B978-0-12-800854-6.00014-2.

Turner, T. R., James, E. K., and Poole, P. S. (2013). The plant microbiome. *Genome Biology* 14, 1–10. doi:10.1186/GB-2013-14-6-209/FIGURES/1.

Udvardi, M., and Poole, P. S. (2013). Transport and Metabolism in Legume-Rhizobia Symbioses. *http://dx.doi.org/10.1146/annurev-arplant-050312-120235* 64, 781–805. doi:10.1146/ANNUREV-ARPLANT-050312-120235.

Ueda, H., Kurose, D., Kugimiya, S., Mitsuhara, I., Yoshida, S., Tabata, J., et al. (2018). Disease severity enhancement by an esterase from non-phytopathogenic yeast Pseudozyma antarctica and its potential as adjuvant for biocontrol agents. *Scientific Reports* 8, 16455. doi:10.1038/s41598-018-34705-z.

Urano, K., Maruyama, K., Koyama, T., Gonzalez, N., Inzé, D., Yamaguchi-Shinozaki, K., et al. (2022). CIN-like TCP13 is essential for plant growth regulation under dehydration stress. *Plant Molecular Biology* 108, 257–275. doi:10.1007/S11103-021-01238-5/FIGURES/9.

Vaid, S. K., Kumar, B., Sharma, A., Shukla, A. K., and Srivastava, P. C. (2014). Effect of zn solubilizing bacteria on growth promotion and zn nutrition of rice. *J Soil Sci Plant Nutr* 14, 889–910. doi:10.4067/S0718-95162014005000071.

Van Den Berg, C., Willemsen, V., Hendriks, G., Weisbeek, P., and Scheres, B. (1997). Short-range control of cell differentiation in the Arabidopsis root meristem. *Nature 1997 390:6657* 390, 287–289. doi:10.1038/36856.

Vega, A., O'Brien, J. A., and Gutiérrez, R. A. (2019). Nitrate and hormonal signaling crosstalk for plant growth and development. *Current Opinion in Plant Biology* 52, 155–163. doi:10.1016/j.pbi.2019.10.001.

Vercruysse, J., Baekelandt, A., Gonzalez, N., and Inzé, D. (2020). Molecular networks regulating cell division during Arabidopsis leaf growth. *J Exp Bot* 71, 2365–2378. doi:10.1093/JXB/ERZ522.

Vogel, C. M., Potthoff, D. B., Schäfer, M., Barandun, N., and Vorholt, J. A. (2021). Protective role of the Arabidopsis leaf microbiota against a bacterial pathogen. *Nature Microbiology 2021 6:12* 6, 1537–1548. doi:10.1038/s41564-021-00997-7.

Vragović, K., Selaa, A., Friedlander-Shani, L., Fridman, Y., Hacham, Y., Holland, N., et al. (2015). Translatome analyses capture of opposing tissuespecific brassinosteroid signals orchestrating root meristem differentiation. *Proc Natl Acad Sci U S A* 112, 923–928. doi:10.1073/PNAS.1417947112/-/DCSUPPLEMENTAL/PNAS.1417947112.SD03.PDF.

Wagner, M. R., Lundberg, D. S., Rio, T. G., Tringe, S. G., Dangl, J. L., and Mitchell-olds, T. (2016). Host genotype and age shape the leaf and root microbiomes of a wild perennial plant. *Nature Communications* 7, 1–15. doi:10.1038/ncomms12151.

Walters, W. A., Jin, Z., Youngblut, N., Wallace, J. G., Sutter, J., Zhang, W., et al. (2018). Large-scale replicated field study of maize rhizosphere identifies heritable microbes. *Proc Natl Acad Sci U S A* 115, 7368–7373. doi:10.1073/pnas.1800918115.

Wang, L., Gu, X., Xu, D., Wang, W., Wang, H., Zeng, M., et al. (2011). miR396-targeted AtGRF transcription factors are required for coordination of cell division and differentiation during leaf development in Arabidopsis. *J Exp Bot* 62, 761–773. doi:10.1093/JXB/ERQ307.

Wickham, H. (2016). *ggplot2: elegant graphics for data analysis*. Springer International Publishing doi:10.1007/978-3-319-24277-4.

Woo, H. R., Koo, H. J., Kim, J., Jeong, H., Yang, J. O., Lee, I. H., et al. (2016). Programming of Plant Leaf Senescence with Temporal and Inter-Organellar Coordination of Transcriptome in Arabidopsis. *Plant Physiology* 171, 452–467. doi:10.1104/PP.15.01929.

Xie, Y., Straub, D., Eguen, T., Brandt, R., Stahl, M., Martínez-García, J. F., et al. (2015). Meta-Analysis of Arabidopsis KANADI1 Direct Target Genes Identifies a Basic Growth-Promoting Module Acting Upstream of Hormonal Signaling Pathways. *Plant Physiology* 169, 1240–1253. doi:10.1104/PP.15.00764.

Yanai, O., Shani, E., Dolezal, K., Tarkowski, P., Sablowski, R., Sandberg, G., et al. (2005). Arabidopsis KNOXI Proteins Activate Cytokinin Biosynthesis. *Current Biology* 15, 1566–1571. doi:10.1016/J.CUB.2005.07.060.

Yu, T., Guan, C., Wang, J., Sajjad, M., Ma, L., and Jiao, Y. (2017). Dynamic patterns of gene expression during leaf initiation. *Journal of Genetics and Genomics* 44, 599–601. doi:10.1016/J.JGG.2017.11.001.

Zamioudis, C., Mastranesti, P., Dhonukshe, P., Blilou, I., and Pieterse, C. M. J. (2013). Unraveling Root Developmental Programs Initiated by Beneficial Pseudomonas spp. Bacteria. *Plant Physiology* 162, 304–318. doi:10.1104/PP.112.212597.

Zhang, J., Liu, Y. X., Zhang, N., Hu, B., Jin, T., Xu, H., et al. (2019). NRT1.1B is associated with root microbiota composition and nitrogen use in field-grown rice. *Nature Biotechnology*. doi:10.1038/s41587-019-0104-4.

Zhao, F., and Traas, J. (2020). Stable establishment of organ polarity occurs several plastochrons before primordium outgrowth in Arabidopsis. *Development (Cambridge)* 148. doi:10.1242/DEV.198820/264800/AM/STABLE-ESTABLISHMENT-OF-ORGAN-POLARITY-SEVERAL.

Zhiponova, M. K., Vanhoutte, I., Boudolf, V., Betti, C., Dhondt, S., Coppens, F., et al. (2013). Brassinosteroid production and signaling differentially control cell division and expansion in the leaf. *New Phytologist* 197, 490–502. doi:10.1111/NPH.12036.